2025 SIDS NDE Joint Programme

Collaborative Research, Development & Demonstration

PRESENTER

Dae-Jin Kim, Ph.D.

UN environment programme | CTCN UN Climate Technology Centre & Network

GRIFFITH UNIVERSITY SOCIAL MARKETING @ GRIFFITH

Microgrid Technology Powered by Renewable Energy & Battery Storage Systems

CONTENTS ...

CONTENTS ...

UN environment programme | CTCN UN Climate Technology Centre & Network

GRIFFITH UNIVERSITY
SOCIAL MARKETING @ GRIFFITH

Introduction to Microgrid

What is a Microgrid?

Microgrid as: “a group of interconnected loads and distributed energy resources (DER) within clearly defined **electrical boundaries** that **act as a single controllable entity** with respect to the grid, and that can connect and disconnect from the grid to enable it to operate in both **‘grid-connected’** and **‘island’** mode.” Source: U.S. Department of Energy (DOE)

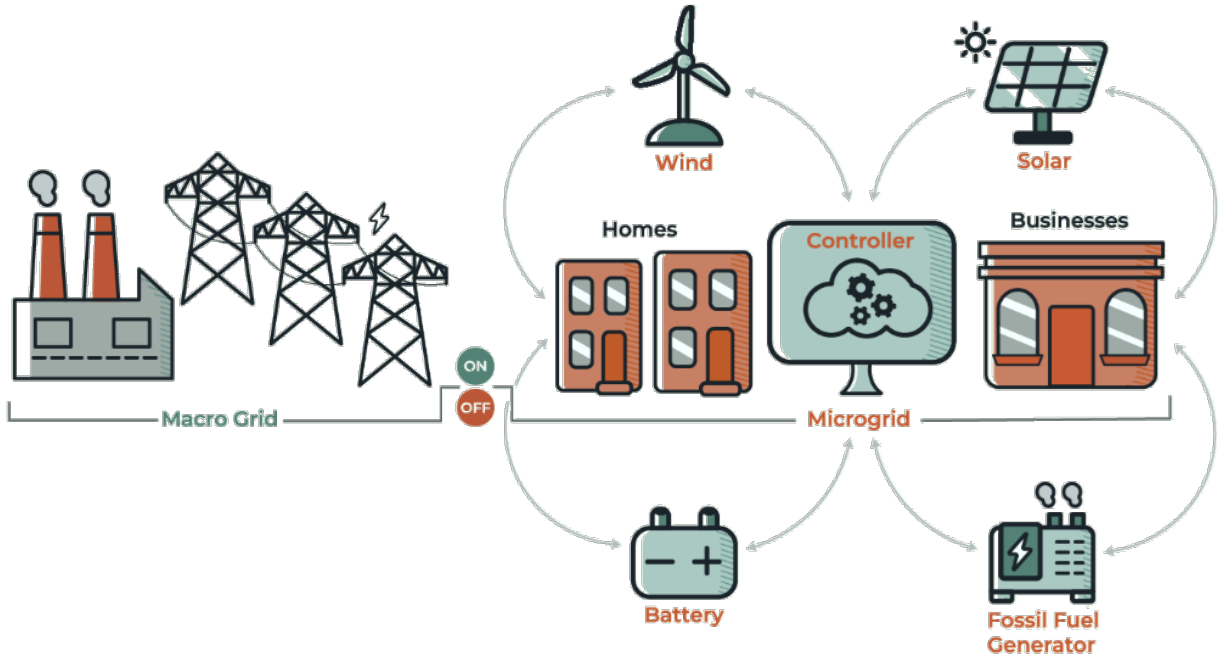

It's **an integrated system of distributed energy resources (DERs)**, such as solar panels and wind turbines, and energy storage systems.

Introduction to Microgrid

What is a Microgrid?

Stand-alone(island) Microgrid

It is typically used in remote or isolated regions such as islands, rural villages, or research bases, where grid extension is technically difficult

Advantages:

- Provides full energy autonomy and independence from the central grid.
- Enhances energy security and resilience, particularly during emergencies or natural disasters.
- Enables local use of renewable resources, reducing reliance on imported fossil fuels.

Limitations:

- Requires sufficient energy storage and backup generation to maintain stable operation.
- Higher capital and operational costs due to storage, redundancy, and control systems.
- More complex design and operation to ensure continuous reliability under varying load and renewable generation.

Grid-connected Microgrid

A grid-connected microgrid is physically and electrically connected to the main utility grid, allowing two-way power exchange. It can operate in parallel with the main grid, and in some cases switch to islanded mode during outages.

Advantages:

- Ensures stable and reliable power supply with support from the utility grid.
- Reduces storage requirements, as the grid can provide balancing power.
- Allows economic benefits through demand response, energy trading, and ancillary services.

Limitations:

- Vulnerable to grid disturbances and failures, reducing resilience in critical situations.
- Lower energy autonomy compared to fully off-grid systems.
- Integration and regulatory issues can be complex, requiring advanced control and protection coordination.

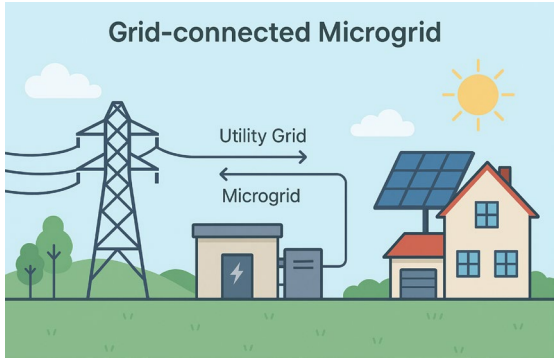

Introduction to Microgrid

What is a Microgrid?

AC Microgrid (AC MG)

An AC microgrid connects distributed generation (PV, wind), storage, and loads through a common AC bus.

- It is compatible with today's existing power systems, since most grids and loads are AC.
- Advantages: Easy integration with the utility grid, mature technologies, and standard protection schemes.
- Limitations: Requires multiple power conversion stages for renewable sources and storage, which increases losses and reduces efficiency.

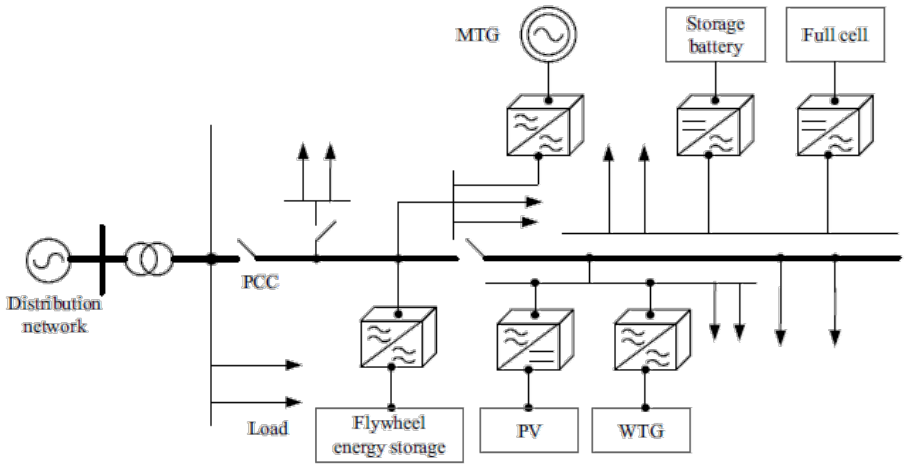

Fig. The topology of AC MG

DC Microgrid (DC MG)

A DC microgrid links distributed resources and storage to a DC bus, then connects to AC systems through converters.

- It is particularly suitable for PV, batteries, EVs, and other native DC devices.
- Advantages: Higher efficiency due to fewer conversion steps, easier integration of renewable energy and storage, and flexible architecture for EV charging or data centers.
- Limitations: Lack of standardized protection methods and less compatibility with the conventional AC grid.

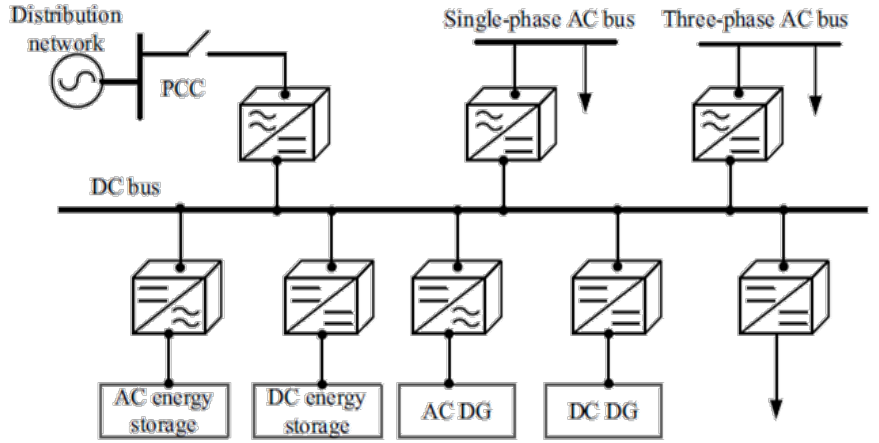

Fig. The topology of DC MG

Source : Stability Analysis, Flexible Control and Optimal Operation of Microgrid, Yong Li, Mingmin Zhang, Yijia Cao Springer Nature Singapore, 2023

Introduction to Microgrid

What is a Microgrid?

Hybrid AC/DC Microgrid

A hybrid microgrid integrates both AC and DC subsystems through a common coupling bus.
It enables simultaneous operation of AC resources such as wind turbines and traditional loads, and DC resources such as PV, batteries, and EV charging stations.

Advantages:

- Maximizes flexibility by allowing both AC and DC devices to connect efficiently.
- Improves overall system efficiency by reducing unnecessary power conversion.
- Enhances resilience by diversifying energy pathways and supporting multiple load types.

Limitations:

- More complex control strategies are required to coordinate power flow between AC and DC sides.
- Protection schemes are more challenging because of different system characteristics.

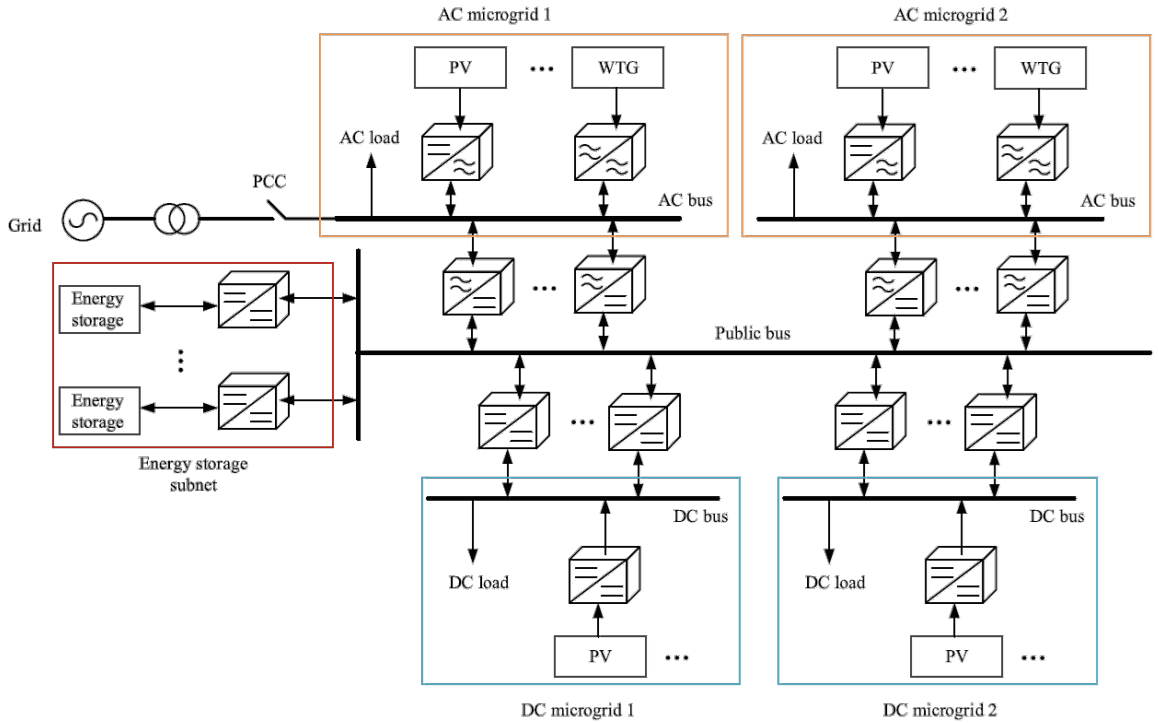

Fig. The topology of hybrid AC/DC MG (AC MG + DC MG)

Source : Stability Analysis, Flexible Control and Optimal Operation of Microgrid, Yong Li, Mingmin Zhang, Yijia Cao Springer Nature Singapore, 2023

Introduction to Microgrid

What is a Microgrid?

CCHP (Combined Cooling, Heating, and Power) Microgrid

A CCHP microgrid integrates renewable power generation (PV, wind) and energy storage with combined thermal energy systems.

This system enables multi-energy supply: power, hot water, and chilled water, all within one integrated microgrid.

Advantages:

- Significantly improves overall energy efficiency by utilizing waste heat from power generation.
- Reduces fuel consumption and emissions.
- Provides greater energy security and flexibility in meeting diverse demands.

Limitations:

- More complex design and operation due to the need to balance electricity, heat, and cooling simultaneously.
- Requires advanced control strategies and precise system coordination.

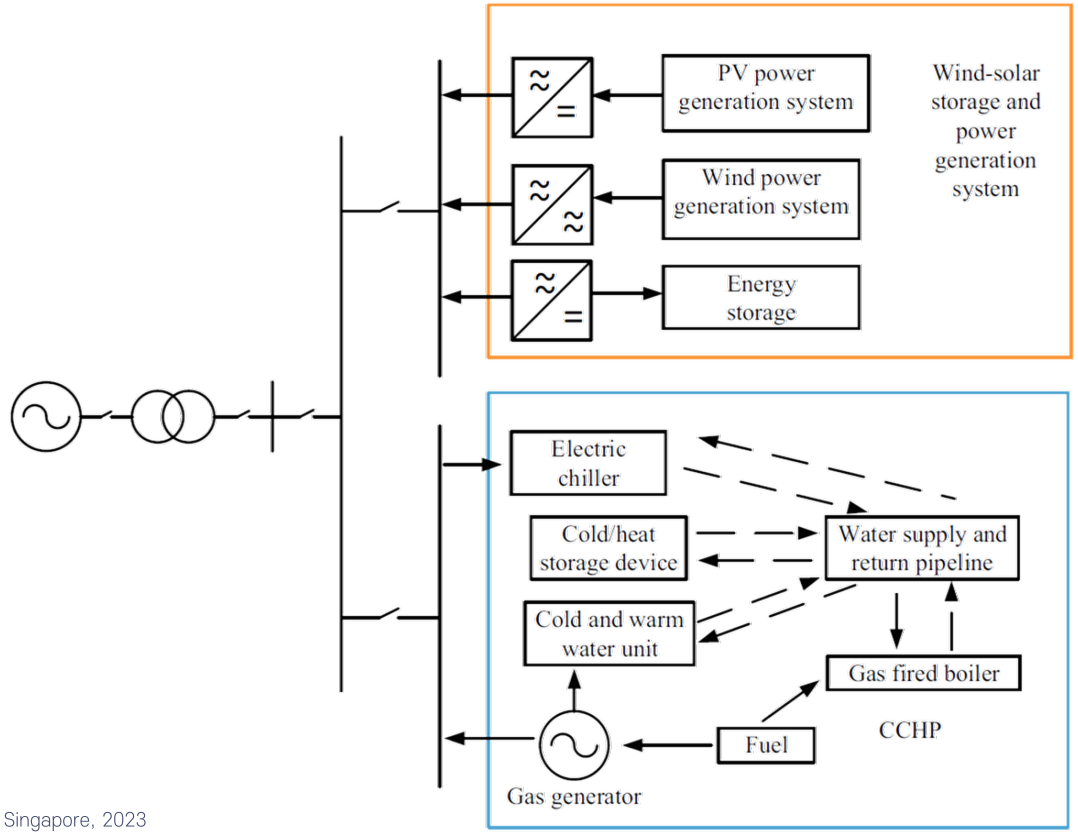

Source : Stability Analysis, Flexible Control and Optimal Operation of Microgrid, Yong Li, Mingmin Zhang, Yijia Cao Springer Nature Singapore, 2023

Fig. The topology of CCHP(Combined Cooling, Heating, and Power)-MG

Introduction to Microgrid

What is a Microgrid?

Stability, Energy Storage Functions, and Optimization in Microgrids

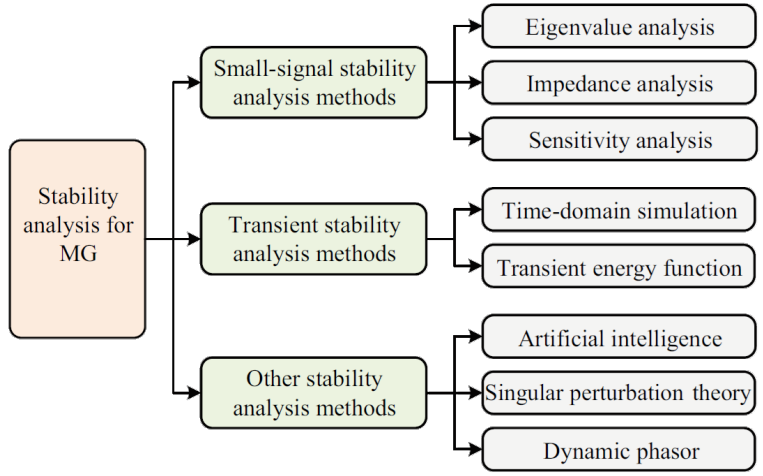

Classification of stability analysis methods in MG

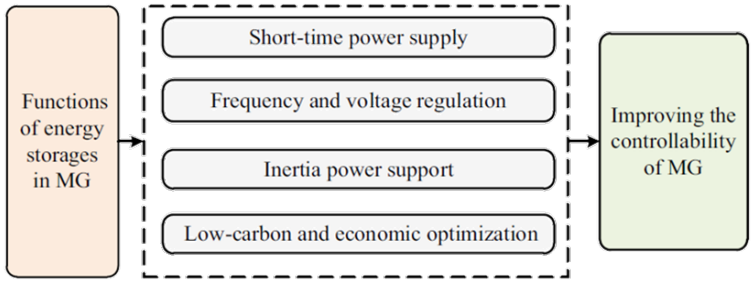

The functions of energy storage systems in MG

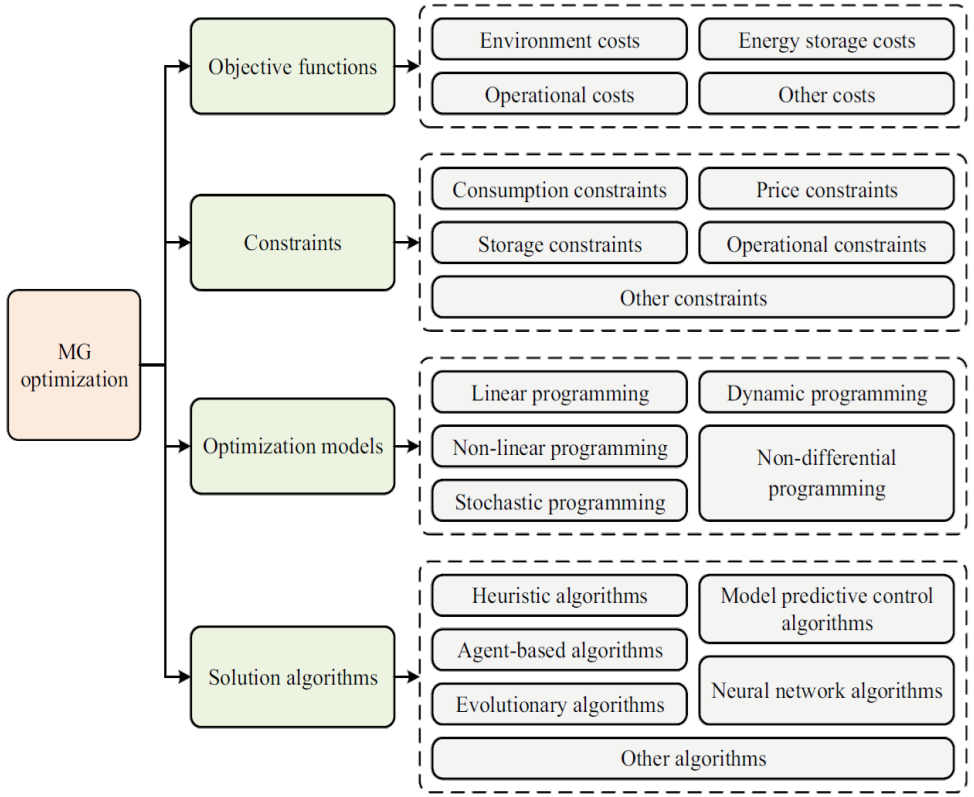

The methodology for optimal operation of MG

Source : Stability Analysis, Flexible Control and Optimal Operation of Microgrid, Yong Li, Mingmin Zhang, Yijia Cao Springer Nature Singapore, 2023

CONTENTS ...

UN environment programme | CTCN UN Climate Technology Centre & Network

GRIFFITH UNIVERSITY
SOCIAL MARKETING @ GRIFFITH

Case study : EV Charging station with RES + BESS

EV Sales and Charging Infrastructure Status

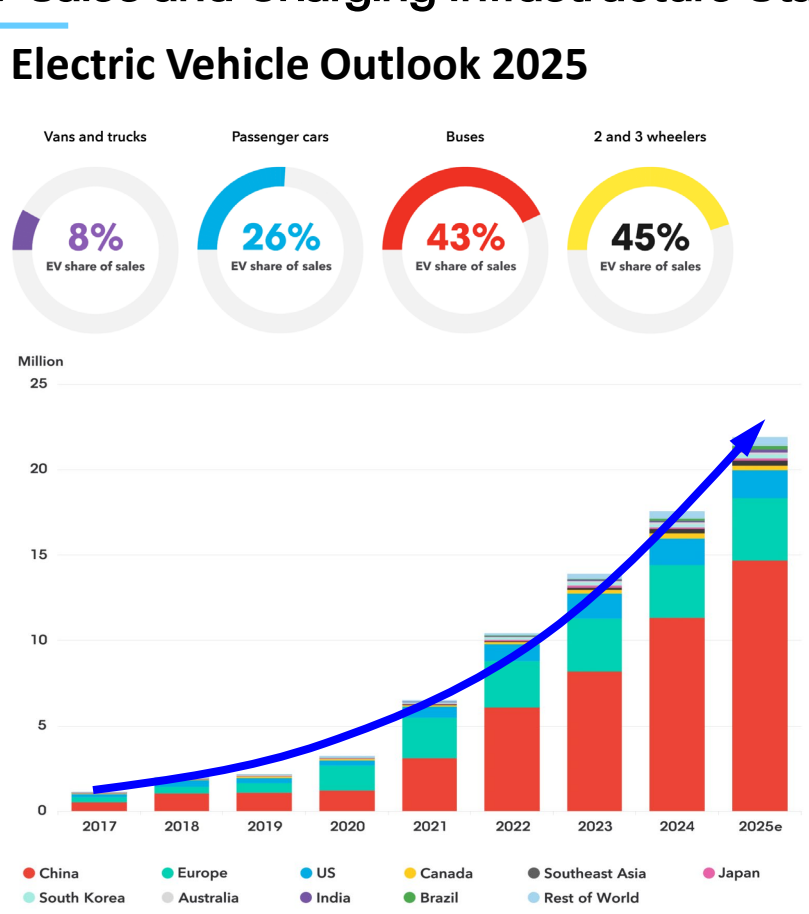

Global Passenger EV Sales by Market

- By 2025, 1 in 4 passenger cars sold worldwide will be electric.
- Some regions show slower EV growth, but automakers continue to expand targets.
- Electrification is also advancing in buses, trucks, and commercial vehicles.

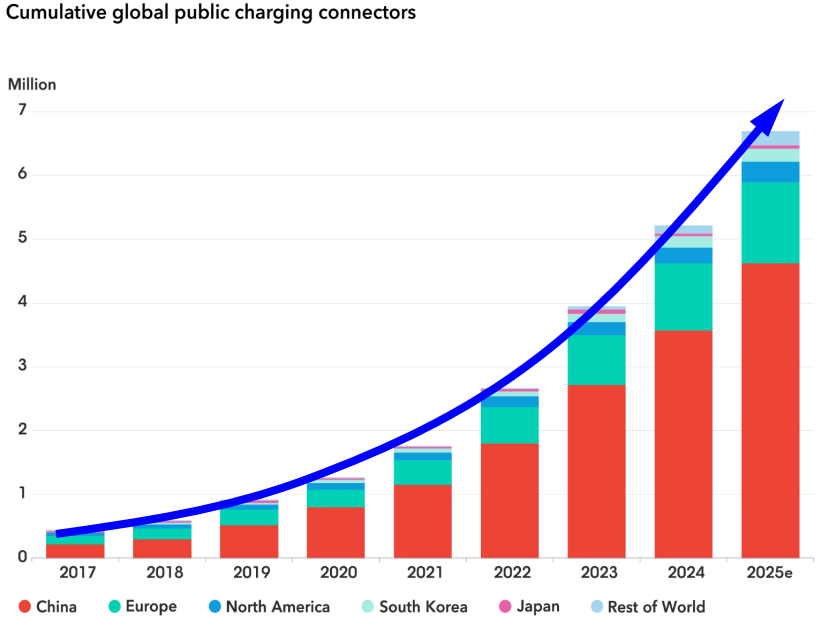

Cumulative Global Public Charging Units

Source : https://about.bnef.com/insights/clean-transport/electric-vehicle-outlook/#key-numbers

Case study : EV Charging station with RES + BESS

EV Sales and Charging Infrastructure Status

Electric Vehicle Supply Equipment (EVSE)

Fig. Slow EVSE (3kW~), AC Power, OBC (Onboard Charger) embedded EV

- Most of them are installed and operated at home.

Fig. Fast EVSE (50kW ~ 350kW), DC Power

- Most of them are installed and operated in public places.

Case study : EV Charging station with RES + BESS

EV Sales and Charging Infrastructure Status

Electric Vehicle Charging Station Market Outlook

- Market value in 2024: USD 39.7 billion
- Global expected CAGR: **24.4% (2025–2034)**
- Projected market size in 2034: approximately USD 363.3 billion

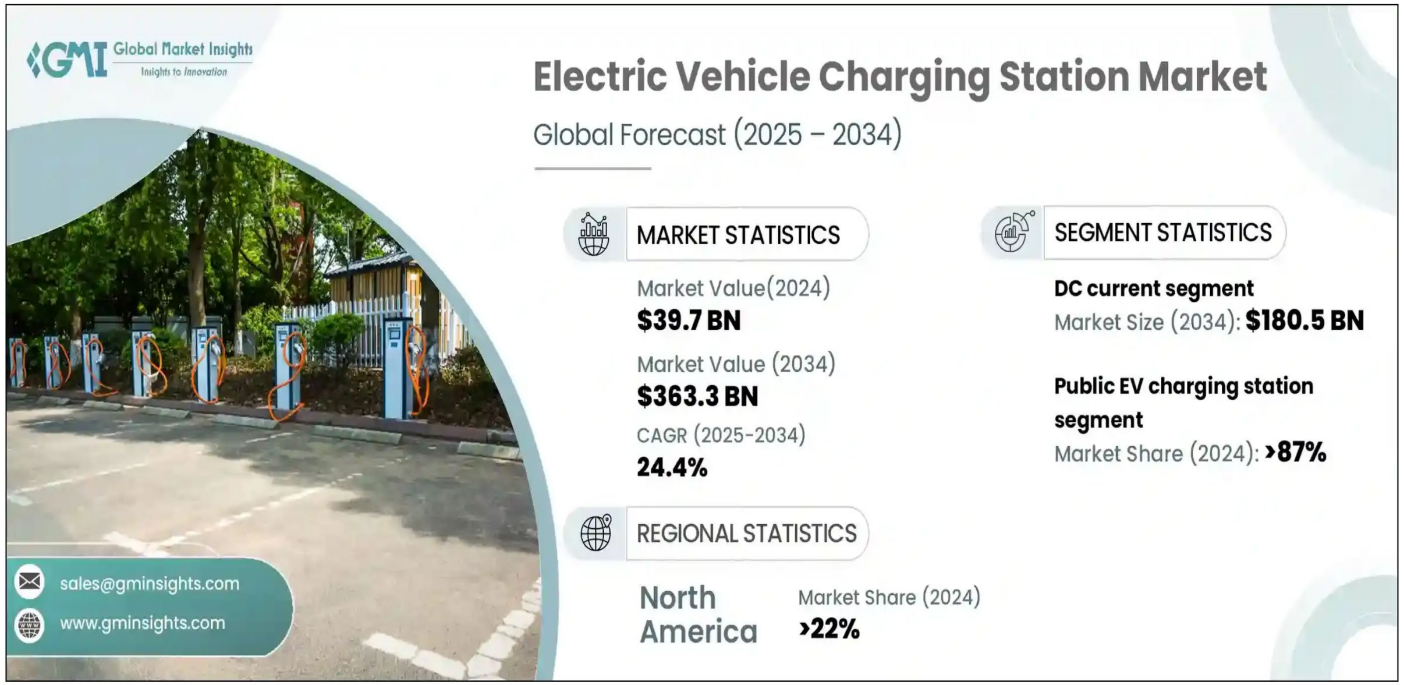

Source : https://www.gminsights.com/ko/industry-analysis/electric-vehicle-charging-station-market

Case study : EV Charging station with RES + BESS

Energy Management System based EV Charging Stations

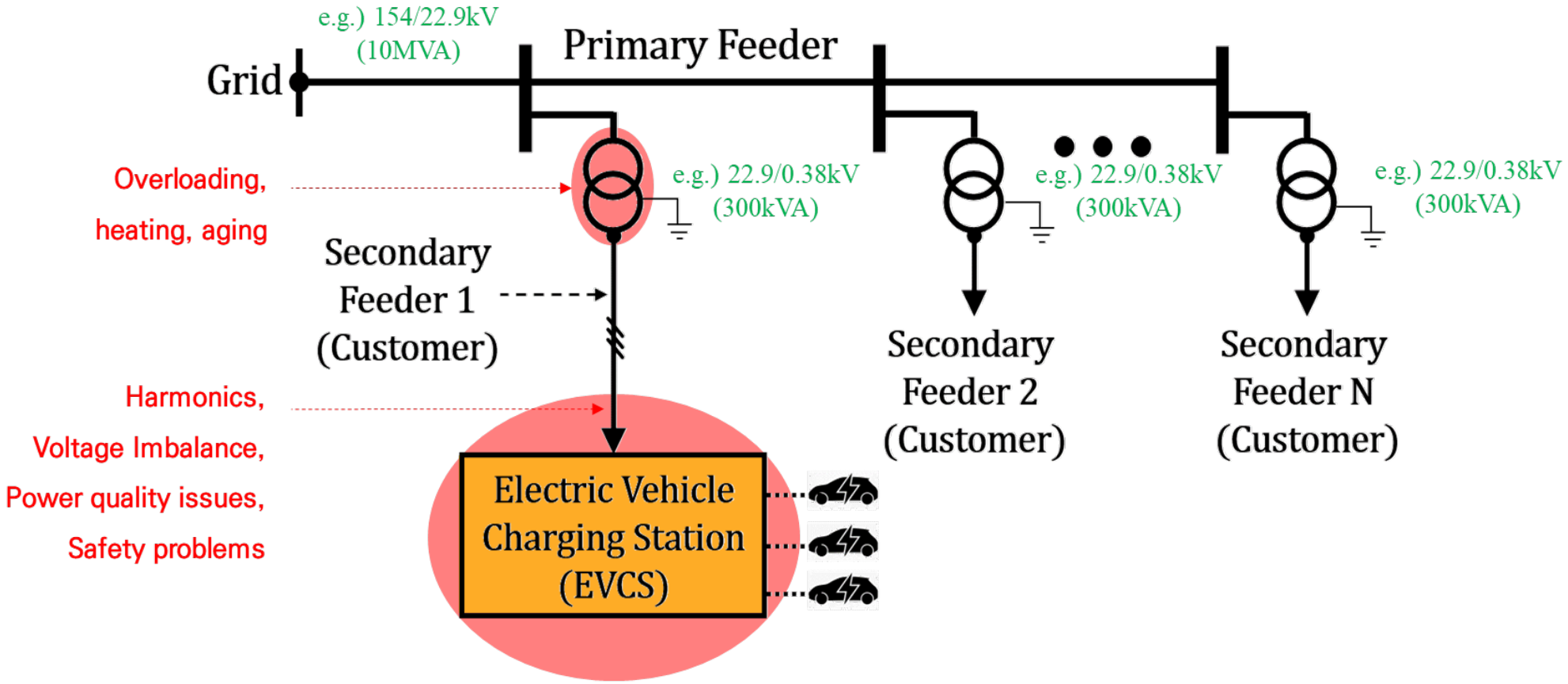

Fig. Electric vehicle charging station (EVCS) in the LV distribution network.

Case study : EV Charging station with RES + BESS

Energy Management System based EV Charging Stations

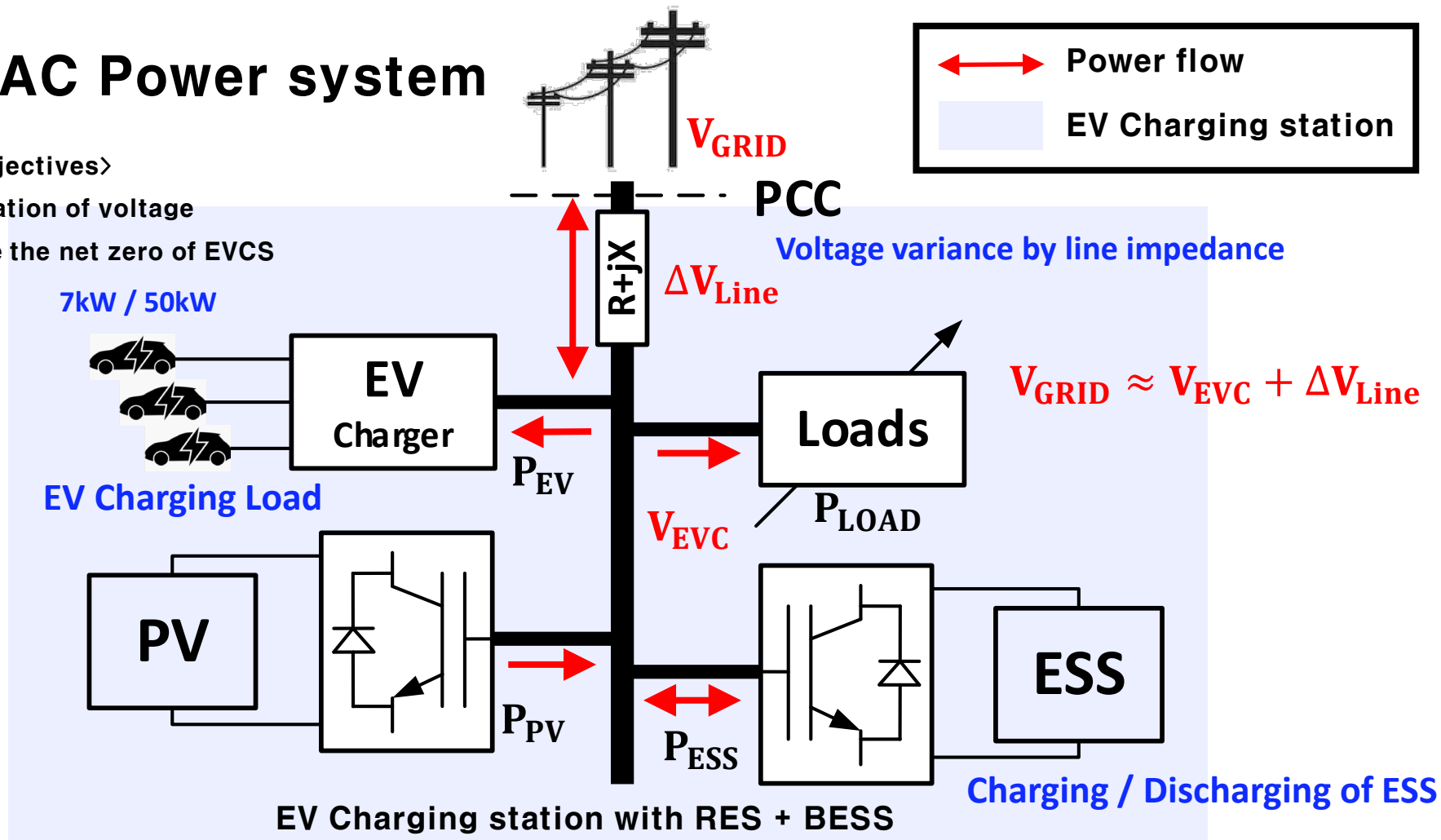

〈Control Objectives〉

- Stabilization of voltage
- Increase the net zero of EVCS

Case study : EV Charging station with RES + BESS

Energy Management System based EV Charging Stations

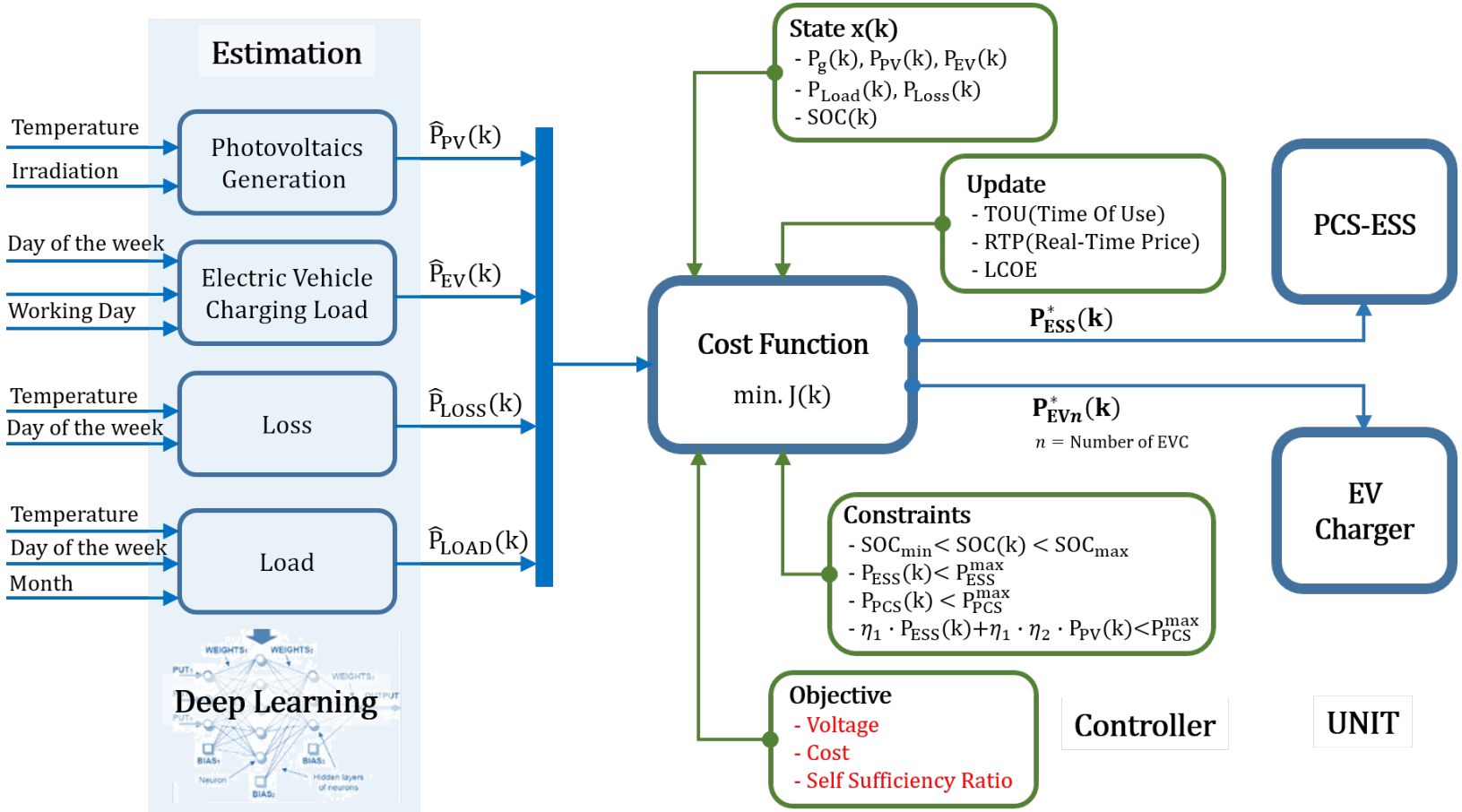

EV Charging Station Operation Algorithm Using Machine Learning

Case study : EV Charging station with RES + BESS

Energy Management System based EV Charging Stations

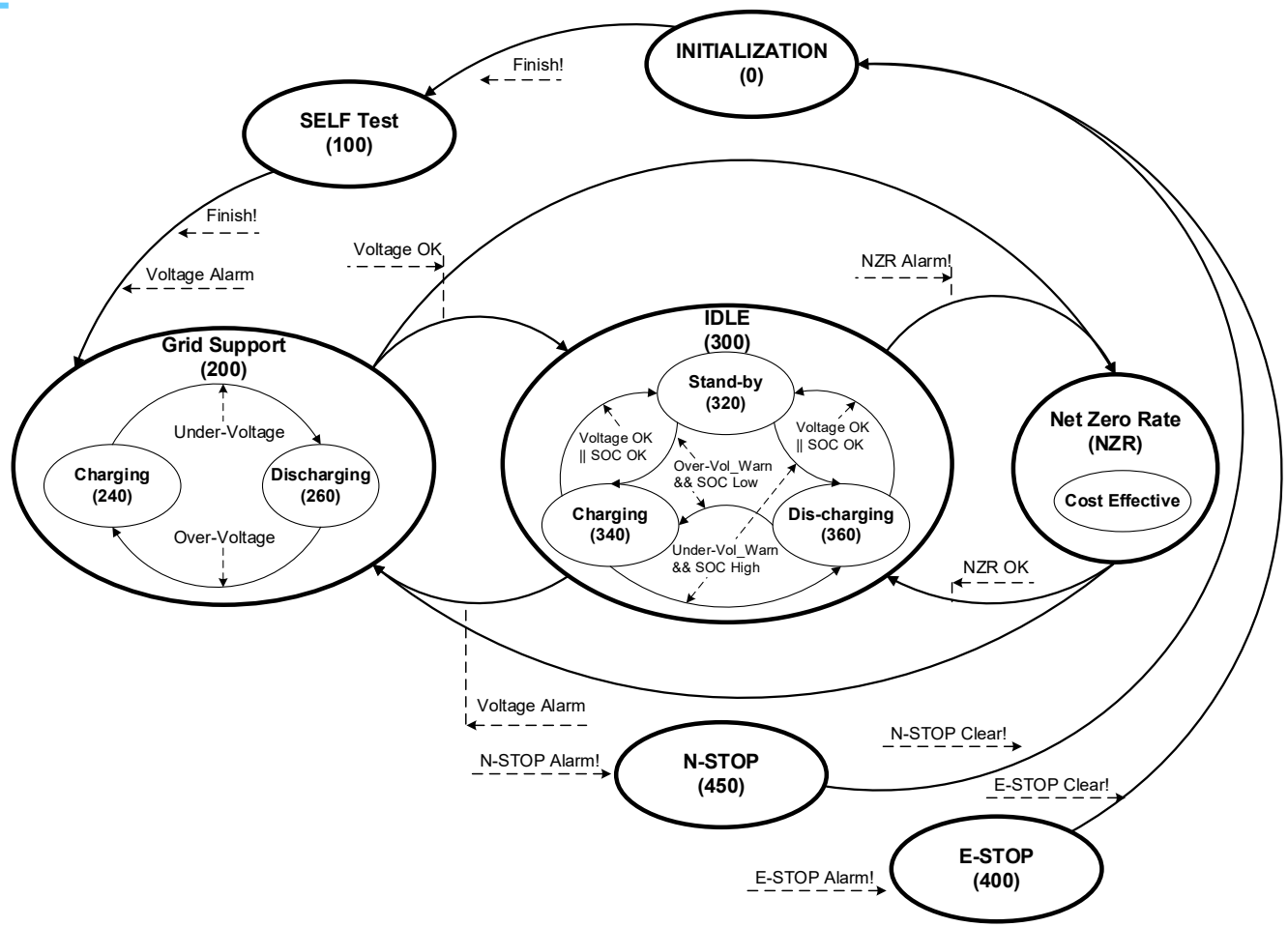

State Machine based control logic of EV Charging station

Case study : EV Charging station with RES + BESS

Energy Management System based EV Charging Stations

PHASOR MODEL (MATLAB/SIMULINK)

- **ESS Hybrid EV Charging station simulation model**
- PHASOR modeling-based simulation.
- 1-day EV charging system simulation (EV, PV, ESS, Load)
- Performance analysis of operation algorithm (baseline data)
- Targets: voltage variation, energy self-sufficiency.

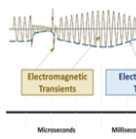

EMT* model / PHASOR Model
(EMT : Electromagnetic Transient)

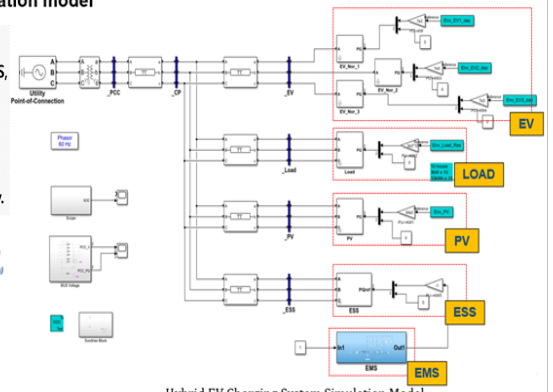

Hybrid EV Charging System Simulation Model
(MATLAB/SIMULINK)

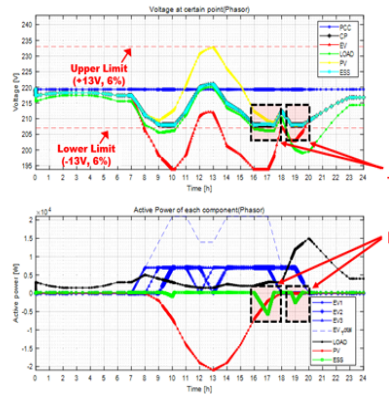

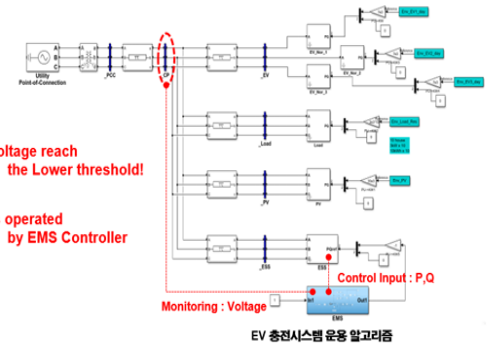

EV 충전시스템 운용 알고리즘

EMTDC[A] MODEL (PSCAD/EMTDC)

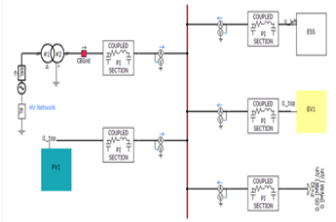

PSCAD/EMTDC 모델링

	완속	급속
Grid	3상 380V_{L-L}	3상 380V_{L-L}
EV	7kW 충전 *2대	50kW
PV	15kW	30kW
BESS	20kWh	100kWh
Load	~100kW	~200kW
LineImpedance	옥외용비닐절연전선(OW)	옥외용비닐절연전선(OW)

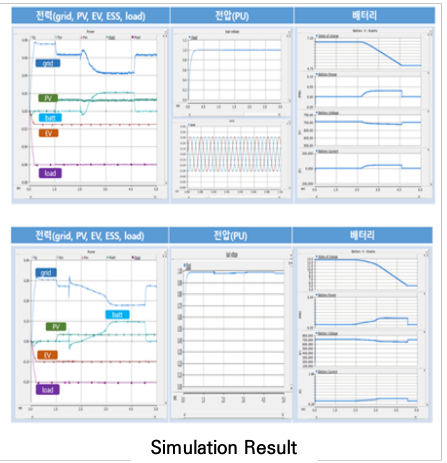

Simulation Result

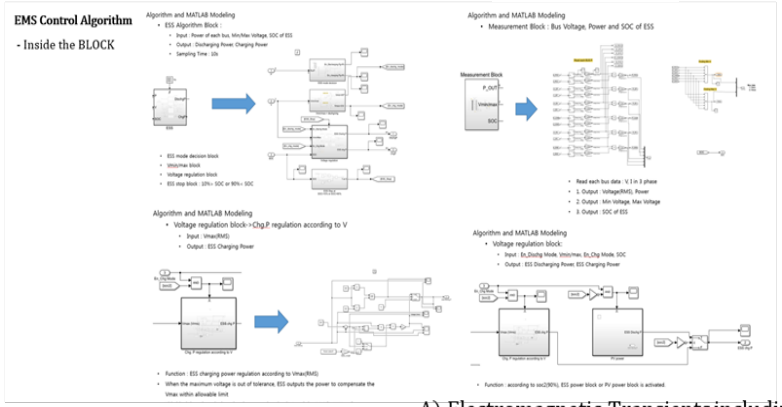

A) Electromagnetic Transients including DC

Case study : EV Charging station with RES + BESS

Energy Management System based EV Charging Stations

- **State-machine based / Control Step Time : 1s / Life signal, Safety**

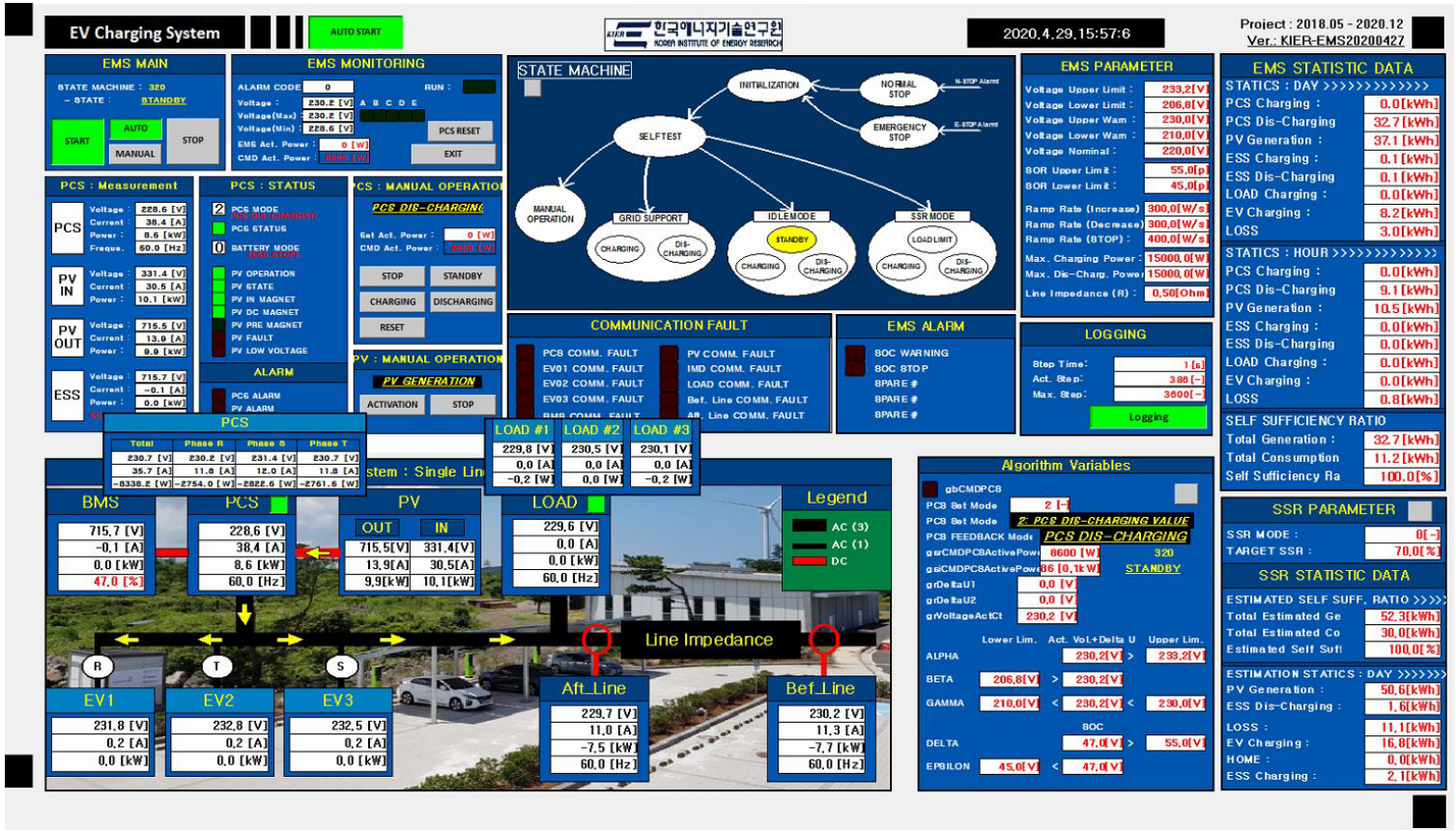

Control system of EV Charging station with RES + BESS

Case study : EV Charging station with RES + BESS

Energy Management System based EV Charging Stations

Open-Platform EVCS
(Electric Vehicle Charging Station)

EV Charging station with RES + BESS (Jeju, Korea Institute of Energy Research)

Case study : EV Charging station with RES + BESS

Energy Management System based EV Charging Stations

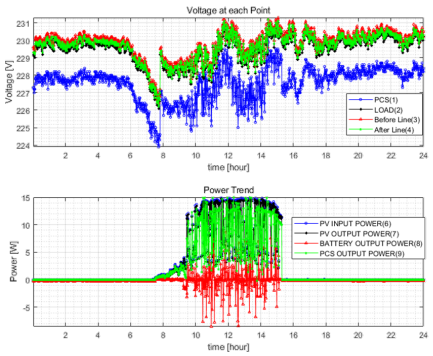

Voltages at each measured point / PV power production

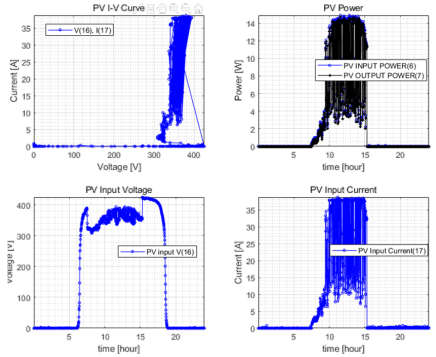

PV Electric measured data (I-V, P-T, V-T, I-A)

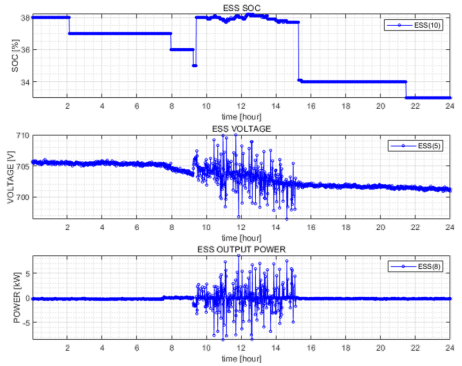

ESS Data (SOC, VOLTAGE, POWER)

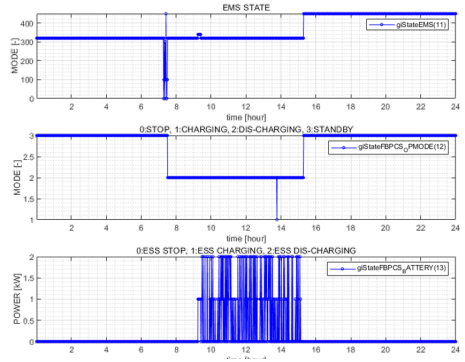

ESS Data (ESS Mode, PCS Mode, Cha./Dis. Mode)

Validate the control algorithm for Voltage stability and Net-zero ratio

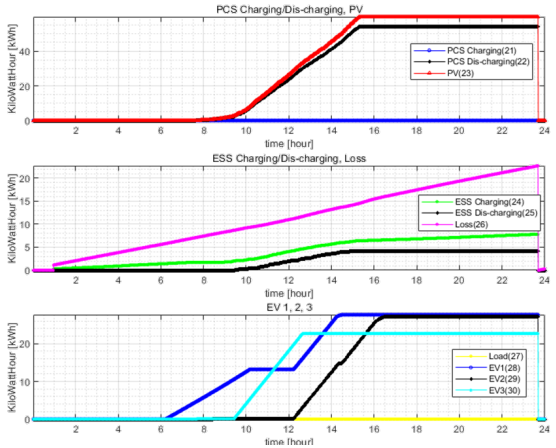

Top : PCS Power, BESS Power (Charging / Discharging)
Bottom : Power of Loads, EV Charging Load 1,2,3

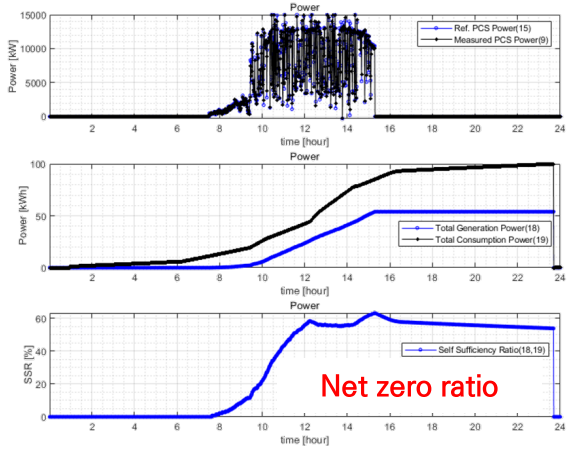

Top : Total generation power / Consumption power
Bottom : Self sufficiency ratio (Net-zero ratio)

Case study : EV Charging station with RES + BESS

Energy Management System based EV Charging Stations

- Completion of hybrid EV charging system testbed and monitoring room construction
- Test operation with parallel load device, distribution board, and PHILS integration
- Development of integrated monitoring system for electrical characteristic analysis
- Preparation of testing procedures for hybrid EV charging infrastructure

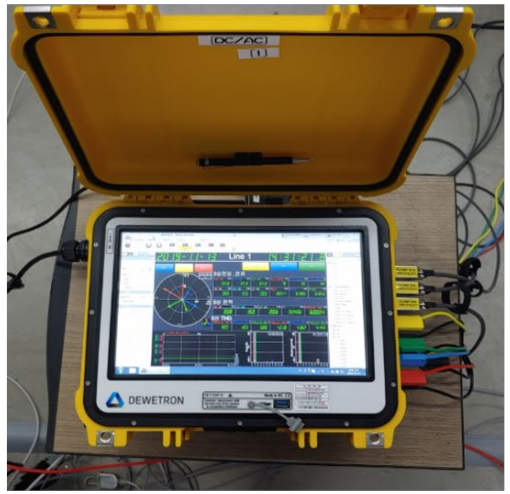

EV charging system simulator (left) / Measurement devices (Dewetron, right)

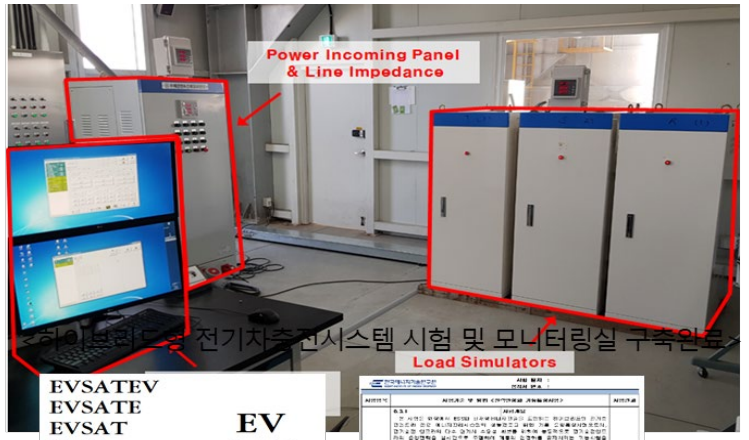

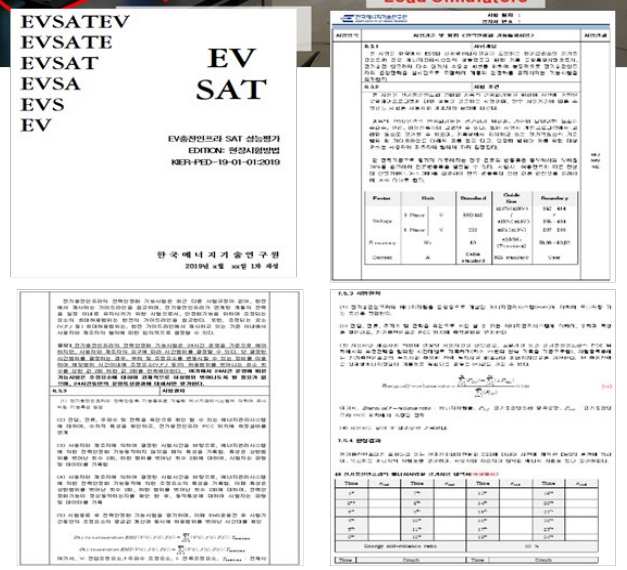

Testing procedures for hybrid EV charging infrastructure

Case study : EV Charging station with RES + BESS

DOB based Model Predictive Voltage Control

Proposed voltage regulation method

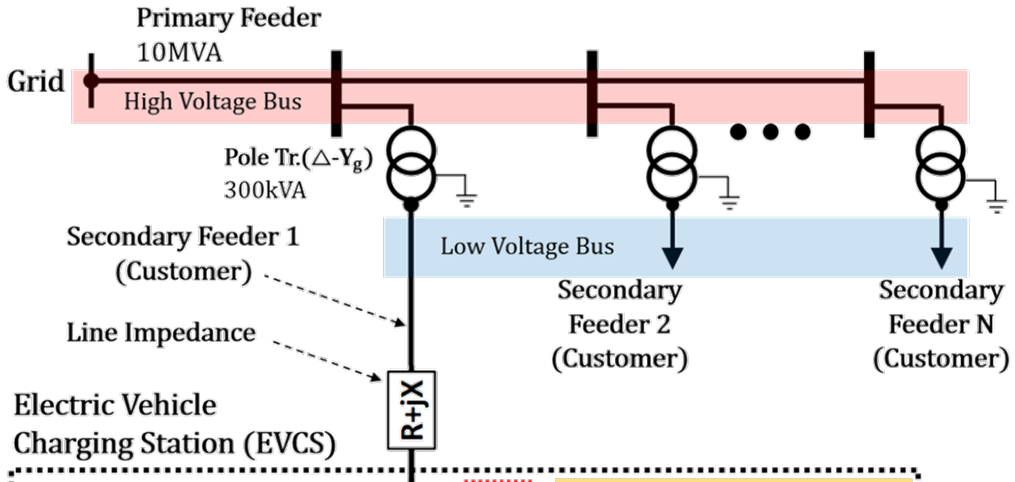

- Model predictive voltage control (MPVC)
- State and disturbance observer
- Obtained the gains by solving LMI-based optimization problem
- Considering parameter uncertainties
- Does not require communication system

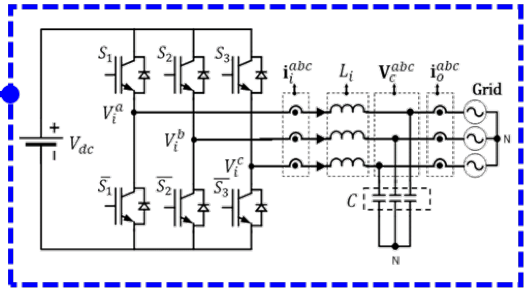

2Level bi-directional Inverter

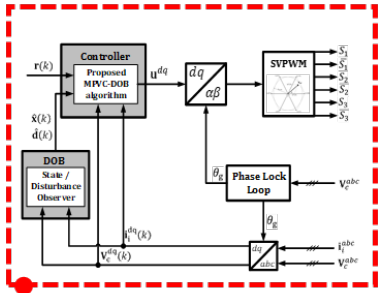

Proposed Method

Case study : EV Charging station with RES + BESS

DOB based Model Predictive Voltage Control

A. Bidirectional Three-phase Inverter with Battery

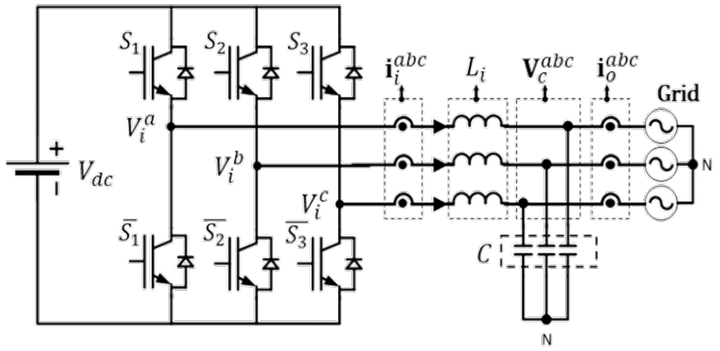

Fig. Three-phase grid-connected inverter with LC filter (battery energy storage systems).

A. Bidirectional Three-phase Inverter with Battery

A three-phase system can be transformed to a synchronous reference frame (SRF)

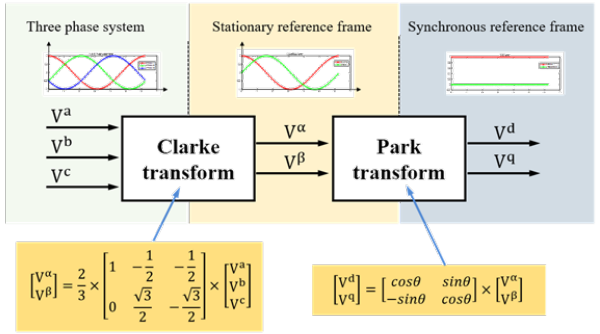

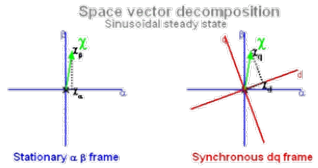

A. Bidirectional Three-phase Inverter with Battery

The system dynamics of the LC filter can be represented by applying Kirchhoff's law as follows:

$$L_i \frac{d\mathbf{i}_i^{abc}}{dt} = \mathbf{V}_i^{abc} - \mathbf{V}_c^{abc} \quad (1)$$

$$C \frac{d\mathbf{V}_c^{abc}}{dt} = \mathbf{i}_i^{abc} - \mathbf{i}_o^{abc} \quad (2)$$

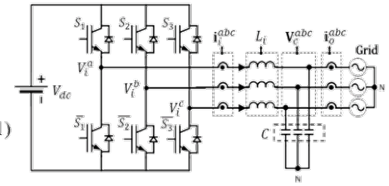

The input voltage $\mathbf{V}_i^{abc}$ can be represented according to [36]:

$$\mathbf{V}_i^{abc} = \frac{1}{6} \begin{bmatrix} 2 & -1 & -1 \\ -1 & 2 & -1 \\ -1 & -1 & 2 \end{bmatrix} \begin{bmatrix} g_1 \\ g_2 \\ g_3 \end{bmatrix} V_{dc} \quad (3)$$

$$g_x = \begin{cases} 1, & S_x = \text{on}; \ \bar{S}_x = \text{off}; \\ -1, & S_x = \text{off}; \ \bar{S}_x = \text{on}; \end{cases} \quad (x = 1, 2, 3)$$

A. Bidirectional Three-phase Inverter with Battery

A three-phase system can be transformed to a synchronous reference frame (SRF). Therefore, (1) and (2) can be expressed in the SRF form [37]:

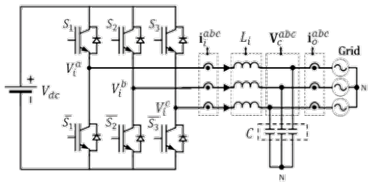

$$\frac{di_i^d}{dt} = \omega i_i^d - \frac{1}{L_i} V_c^d + \frac{1}{L_i} V_i^d \quad (4)$$

$$\frac{di_i^q}{dt} = -\omega i_i^q - \frac{1}{L_i} V_c^q + \frac{1}{L_i} V_i^q \quad (5)$$

$$\frac{dV_c^d}{dt} = \frac{1}{C} i_i^d + \omega V_c^q - \frac{1}{C} i_o^d \quad (6)$$

$$\frac{dV_c^q}{dt} = \frac{1}{C} i_i^q - \omega V_c^d - \frac{1}{C} i_o^q \quad (7)$$

Case study : EV Charging station with RES + BESS

DOB based Model Predictive Voltage Control

B. Low Voltage Distribution Network

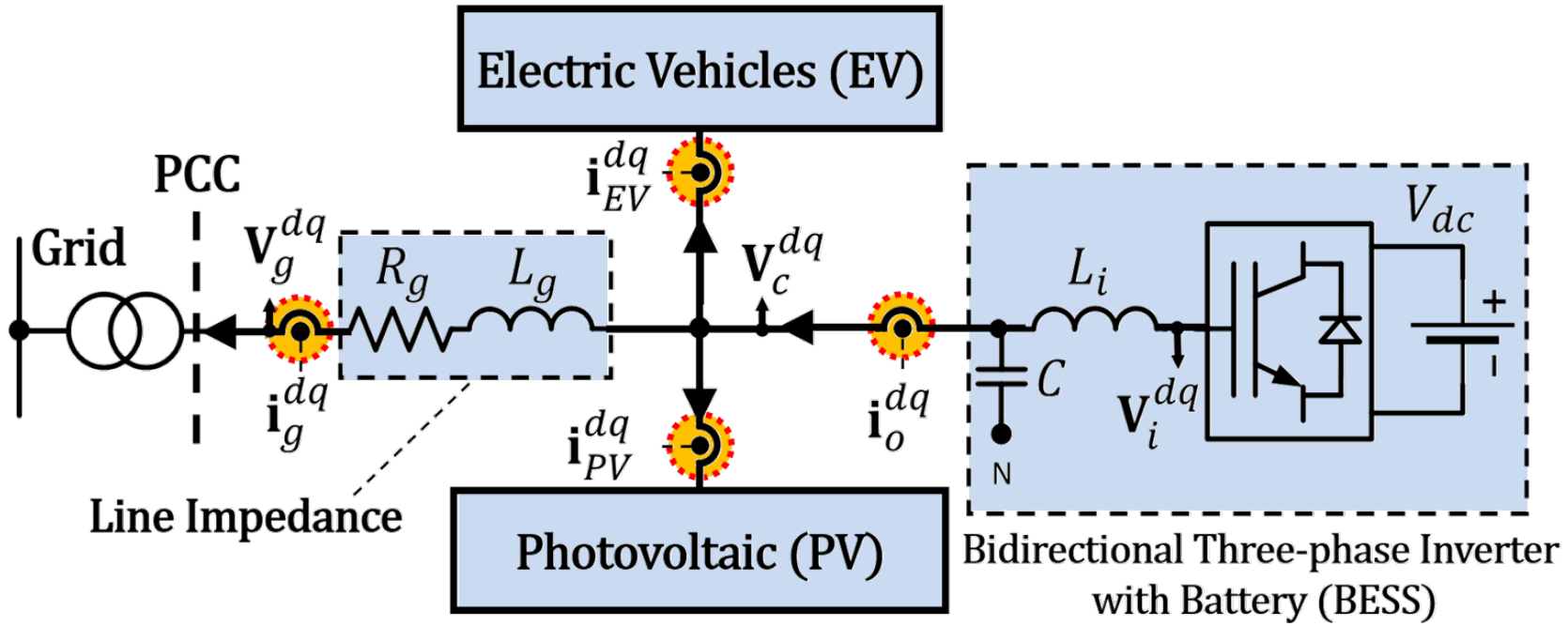

Fig. Electric vehicle charging station (EVCS) with line impedance in the low-voltage distribution network.

Case study : EV Charging station with RES + BESS

DOB based Model Predictive Voltage Control

A. State and Disturbance Observer Design

The unknown disturbance current $\mathbf{d}(k)$ is assumed to be constant as follows:

$$\mathbf{d}(k+1) = \mathbf{d}(k) \tag{18}$$

$$\hat{\mathbf{d}}(k+1) = \hat{\mathbf{d}}(k) + \mathbf{L}_2(\mathbf{y}(k) - \hat{\mathbf{y}}(k)) \tag{19}$$

The state observer is proposed as follows using the observed disturbance $\hat{\mathbf{d}}$:

$$\begin{aligned}\hat{\mathbf{x}}(k+1) = {} & \mathbf{A}\hat{\mathbf{x}}(k) + \mathbf{B}\mathbf{u}(k) \\ & + \mathbf{L}_1(\mathbf{y} - \mathbf{C}\hat{\mathbf{x}}) + \mathbf{B}_d\hat{\mathbf{d}}(k) + \mathbf{B}_g\mathbf{V}_g(k)\end{aligned} \tag{20}$$

where $\mathbf{V}_g(k)$ is the grid voltage at the point of common coupling and is assumed to be directly connected to the secondary side of the transformer. Therefore, $\mathbf{V}_g(k)$ was considered as a constant value.

Asymptotic stability

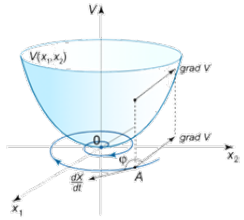

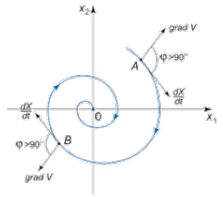

A Lyapunov global asymptotic stability theorem (Lyapunov's second method for stability)

suppose there is a function $\mathrm{V}(x)$ such that

- $\mathrm{V}(x) = 0$ *if and only if* $x = 0$
- $\mathrm{V}(x) > 0$ *if and only if* $x \neq 0$
- $\dot{\mathrm{V}}(x) < 0$

then, every trajectory of $\dot{x} = f(x)$ converges to zero as $t \to \infty$.

Continuous−time domain	Discrete−time domain
$\dot{\mathrm{V}}(x) < 0, \mathrm{V}(x) > 0 (x \neq 0), \mathrm{V}(0) = 0$	$\mathrm{V}(k+1) - \mathrm{V}(k) < 0, \mathrm{V}(k) > 0$
$\mathrm{V}(x) \coloneqq x(t)^{\mathrm{T}}\mathrm{P}x(t)$	$\mathrm{V}(k) \coloneqq \mathrm{x}(k)^{\mathrm{T}}\mathrm{P}\mathrm{x}(k)$
$\dot{x}(\mathrm{t}) = \mathrm{A}x(t)$	$\mathrm{V}(k+1) = \mathrm{x}(k+1)^{\mathrm{T}}\mathrm{P}\mathrm{x}(k+1)$
$\dot{\mathrm{V}}(x) = x(t)^{\mathrm{T}}(\mathrm{A}^{\mathrm{T}}\mathrm{P} + \mathrm{PA})x(t) < 0$	where $\mathrm{x}(k+1) = \mathrm{A}\mathrm{x}(k)$.
$\mathrm{A}^{\mathrm{T}}\mathrm{P} + \mathrm{PA} < 0$	$\mathrm{V}(k+1) - \mathrm{V}(k) = \mathrm{x}(k)^{\mathrm{T}}(\mathrm{A}^{\mathrm{T}}\mathrm{PA} - \mathrm{P})\mathrm{x}(k) < 0$
	$\mathrm{A}^{\mathrm{T}}\mathrm{PA} - \mathrm{P} < 0$

A. State and Disturbance Observer Design

Subtracting (20) from (17) and (19) from (18), we obtain the following

$$\mathbf{g}(k+1) = [\mathbf{A}_e - \mathbf{L}\mathbf{C}_e]\mathbf{g}(k) \tag{21}$$

where

$\tilde{\mathbf{x}}(k+1) \coloneqq \mathbf{x}(k+1) - \hat{\mathbf{x}}(k+1)$ and

$\tilde{\mathbf{d}}(k+1) \coloneqq \mathbf{d}(k+1) - \hat{\mathbf{d}}(k+1)$.

$$\mathbf{g}(k) \coloneqq \begin{bmatrix}\tilde{\mathbf{x}}(k) \\ \tilde{\mathbf{d}}(k)\end{bmatrix} \mathbf{A}_e \coloneqq \begin{bmatrix}\mathbf{A} & \mathbf{B}_d \\ \mathbf{0}_{2\mathrm{x}6} & \mathbf{I}_{2\mathrm{x}2}\end{bmatrix}, \mathbf{L} \coloneqq \begin{bmatrix}\mathbf{L}_1 \\ \mathbf{L}_2\end{bmatrix}, \mathbf{C}_e \coloneqq [\mathbf{C}\ \ \mathbf{0}_{2\mathrm{x}2}].$$

Suppose that a Lyapunov function is defined as

$$V(k) = \mathbf{g}(k)^T\mathbf{P}\mathbf{g}(k) \tag{22}$$

where $\mathbf{P}$ is a positive definite matrix.

A. State and Disturbance Observer Design

The observer gain $\mathbf{L}$ is determined such that $V(k)$ of (22) decreases monotonically as follows [36]:

$$\begin{aligned}& V(k+1) - V(k) \\ & = \mathbf{g}(k)^T\left([\mathbf{A}_e - \mathbf{L}\mathbf{C}_e]^T\mathbf{P}[\mathbf{A}_e - \mathbf{L}\mathbf{C}_e] - \mathbf{P}\right)\mathbf{g}(k) < 0\end{aligned} \tag{23}$$

Equation (23) is satisfied for all nonzero $\mathbf{g}(k)$ when

$$[\mathbf{A}_e - \mathbf{L}\mathbf{C}_e]^T\mathbf{P}[\mathbf{A}_e - \mathbf{L}\mathbf{C}_e] - \mathbf{P} < 0 \tag{24}$$

is satisfied. It is clear that (24) holds if for some $\mathbf{P}_o > 0$ $(\mathbf{P} > \mathbf{P}_o)$

$$\mathbf{P}_o - [\mathbf{P}\mathbf{A}_e - \mathbf{P}\mathbf{L}\mathbf{C}_e]^T\mathbf{P}^{-1}[\mathbf{P}\mathbf{A}_e - \mathbf{P}\mathbf{L}\mathbf{C}_e] > 0 \tag{25}$$

is fulfilled.

Case study : EV Charging station with RES + BESS

DOB based Model Predictive Voltage Control

The cost function $J(k)$ is defined as follows using $\mathbf{x_0}$ and $\mathbf{u_0}$ obtained from (33–39):

$$J(k) := \|\hat{\mathbf{e}}(k+1)\|_{\mathbf{H}} + \|\Delta\mathbf{u}(k)\|_{\mathbf{R}}, \quad (41)$$

where

$$\hat{\mathbf{e}}(k+1) := \hat{\mathbf{x}}(k+1) - \mathbf{x}_0(k+1),$$

$$\Delta\mathbf{u} := \mathbf{u}(k) - \mathbf{u_0},$$

$$\|\boldsymbol{x}\|_{\mathbf{H}} := \boldsymbol{x}^{\boldsymbol{T}}\mathbf{H}\boldsymbol{x}, \text{ and } \mathbf{H} > 0,\ \mathbf{R} > 0.$$

A. Reference Steady State

The steady-state $\mathbf{x}_0$ of system (17) satisfies the following relationship:

$$\mathbf{x}(k+1) = \mathbf{A}\mathbf{x}(k) + \mathbf{B}\mathbf{u}(k) + \mathbf{B}_d\mathbf{d}(k) + \mathbf{B}_g\mathbf{V}_g(k) \quad (17)$$

$$\mathbf{x}_0 = \mathbf{A}\mathbf{x}_0 + \mathbf{B}\mathbf{u}_0 + \mathbf{B}_d\mathbf{d}(k) + \mathbf{B}_g\mathbf{V}_g(k), \quad (32)$$

where

$$\mathbf{x_0} = [i_i^{d^o}\ \ i_i^{q^o}\ \ V_c^{d^*}\ \ V_c^{q^*}\ \ i_g^{d^o}\ \ i_g^{q^o}]^{\mathrm{T}},$$
$$\mathbf{u}_0 = [V_i^{d^o}\ \ V_i^{q^o}]^{\mathrm{T}}$$

Note that the disturbance $\mathbf{d}$ is not measurable and will be replaced by $\hat{\mathbf{d}}(k)$ at each time step to yield

$$\mathbf{x}_0 = \mathbf{A}\mathbf{x}_0 + \mathbf{B}\mathbf{u}_0 + \mathbf{B}_d\hat{\mathbf{d}}(k) + \mathbf{B}_g\mathbf{V}_g \quad (33)$$

<Variables>

- $\hat{x}(k)$: estimated state
- x_0: state at normal state
- $u(k)$: Control input a
- $u_0(k)$: Control input at normal state

B. Design of model predictive voltage control

The cost function $J(k)$ is defined as follows using $\mathbf{x_0}$ and $\mathbf{u_0}$ obtained from (33–39):

$$J(k) := \|\hat{\mathbf{e}}(k+1)\|_{\mathbf{H}} + \|\Delta\mathbf{u}(k)\|_{\mathbf{R}}, \quad (41)$$

where

$$\hat{\mathbf{e}}(k+1) := \hat{\mathbf{x}}(k+1) - \mathbf{x}_0(k+1), \Delta\mathbf{u} := \mathbf{u}(k) - \mathbf{u_0},$$
$$\|\boldsymbol{x}\|_{\mathbf{H}} := \boldsymbol{x}^{\boldsymbol{T}}\mathbf{H}\boldsymbol{x}, \text{ and } \mathbf{H} > 0,\ \mathbf{R} > 0.$$

To minimize the cost function $J(k)$, we use the following control law:

$$\Delta\mathbf{u}(k) = \mathbf{K}\hat{\mathbf{e}}(k). \quad (42)$$

Inserting (20) and (33) into $\hat{\mathbf{e}}(k+1)$, we have

$$\begin{aligned}\hat{\mathbf{e}}(k+1) &= \hat{\mathbf{x}}(k+1) - \mathbf{x}_0(k) \\ &= \mathbf{A}\hat{\mathbf{x}}(k) + \mathbf{B}\mathbf{u}(k) + \mathbf{L_1}(\mathbf{y} - \mathbf{C}\hat{\mathbf{x}}) - \mathbf{A}\mathbf{x_0}(k) - \mathbf{B}\mathbf{u_0}(k).\end{aligned} \quad (43)$$

Case study : EV Charging station with RES + BESS

DOB based Model Predictive Voltage Control

D. Stability analysis of observer and controller

To verify the stability of the closed-loop system, substitution of the controller (43) into (20) and use of $\tilde{\mathbf{x}}(k)$ from (21) yields

$$\mathbf{z}(k+1) = \mathbf{A}_{cl}\mathbf{z}(k) + \begin{bmatrix}\mathbf{B}\\ \mathbf{0}_{6x2}\end{bmatrix}\mathbf{u}_0 + \begin{bmatrix}\mathbf{B}_d & \mathbf{0}_{6x2}\\ \mathbf{0}_{6x2} & \mathbf{B}_d\end{bmatrix}\begin{bmatrix}\mathbf{d}(k)\\ \tilde{\mathbf{d}}(k)\end{bmatrix} + \begin{bmatrix}\mathbf{B}_g\\ \mathbf{0}_{6x2}\end{bmatrix}\mathbf{V}_g(k) \quad (55)$$

where

$$\mathbf{z}(k) := \begin{bmatrix}\mathbf{x}(k)\\ \tilde{\mathbf{x}}(k)\end{bmatrix}, \mathbf{A}_{cl} := \begin{bmatrix}\mathbf{A}+\mathbf{BK} & -\mathbf{BK}\\ \mathbf{0}_{6x6} & \mathbf{A}-\mathbf{L}_1\mathbf{C}\end{bmatrix}.$$

From (55), it is clear that the overall stability is determined by the stabilities of $\mathbf{A}+\mathbf{BK}$ and $\mathbf{A}-\mathbf{L}_1\mathbf{C}$, which are ensured by (47) and (24), respectively.

D. Stability analysis of observer and controller

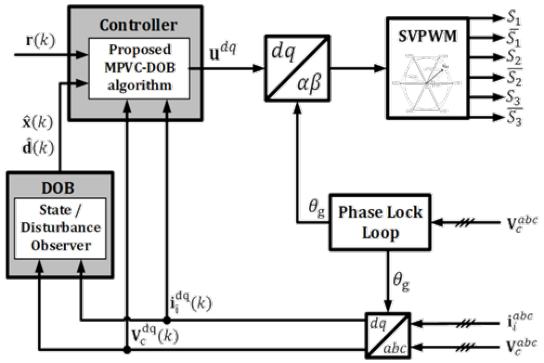

Fig. Block diagram of the proposed model predictive voltage control (MPVC) scheme with disturbance observer.

D. Stability analysis of observer and controller

To verify the stability of the closed-loop system, substitution of the controller (43) into (20) and use of $\tilde{\mathbf{x}}(k)$ from (21) yields

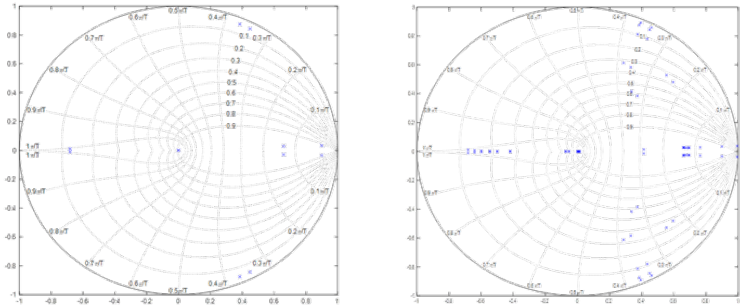

(a) (b)

Fig. Poles $\mathbf{A}_{cl}$ of closed-loop system in z-domain. (a) with nominal parameters, (b) with parameter uncertainties (μ =1.0, 1.1, 1.5, 2.0, 2.5).

Model Predictive Voltage Control (MPVC)

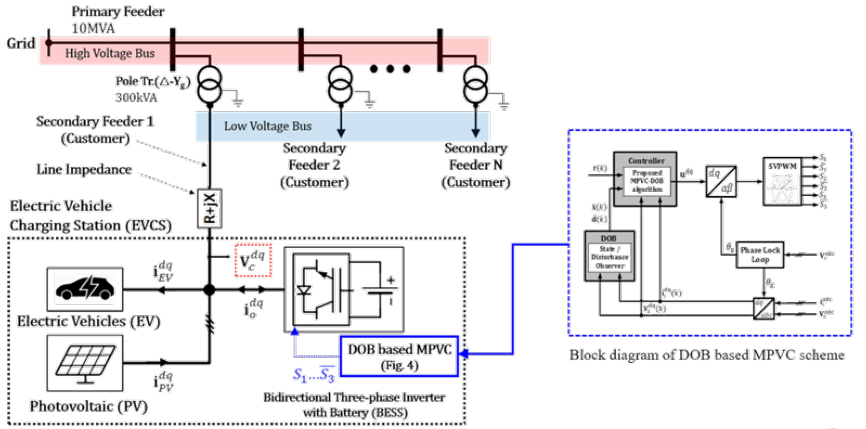

Block diagram of DOB based MPVC scheme

Fig. Segment of a distribution network with EVCS that applies DOB-based MPVC to BESS.

Case study : EV Charging station with RES + BESS

DOB based Model Predictive Voltage Control

Overall experimental environment of EVCS.

Line Impedance Simulator / Load Simulator

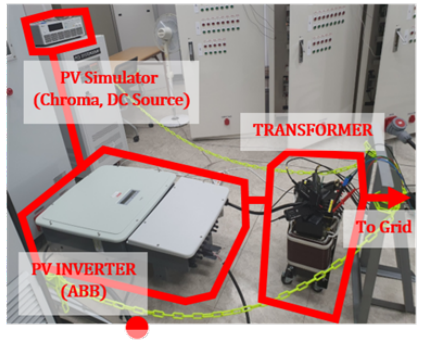

PV Simulator with PV Inverter

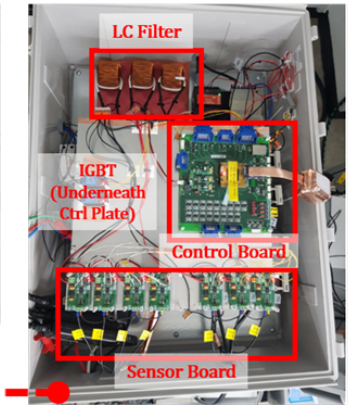

Bidirectional Three Phase Inverter

Grid Simulator

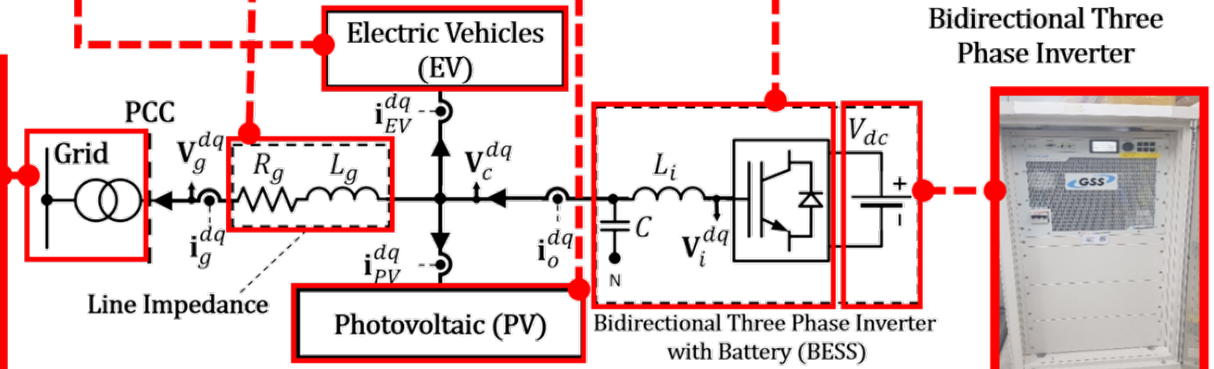

Battery Simulator

Experimental environment of EVCS with proposed bidirectional inverter

- CASE #1 : 2kW EV charging load with step input
  - *d-q* axis : Event : EV charging load at 10.5 s.
  - Performance on $\mathbf{V}_c^{dq}$ voltage regulation
  - 3 phase voltage : Event : EV charging load at 10.5 s.

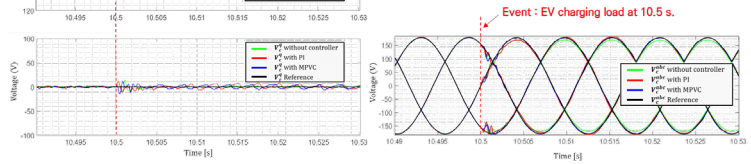

Fig. Comparisons of the performances of PI and MPVC when the 2kW EV charging load is applied to EVCS.

- CASE #2 : 2.5kW PV generation power
  - *d-q* axis : Event : PV generation power at 8.0 s.
  - Performance on $\mathbf{V}_c^{dq}$ voltage regulation
  - 3 phase voltage : Event : PV generation power at 8.0 s.

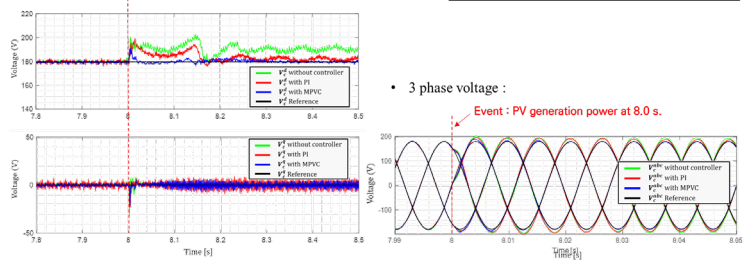

Fig. Comparisons of the performances of PI and MPVC when the 2.5kW PV power generation is applied to EVCS.

- CASE #1 : 2kW EV charging load with step input
  - Performance on disturbance observer
  - Event : EV charging load at 10.5 s.
- CASE #2 : 2.5kW PV generation power
  - Performance on disturbance observer
  - Event : PV generation power at 8.0 s.

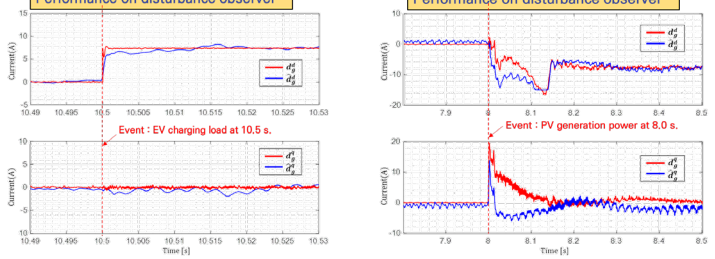

Case study : EV Charging station with RES + BESS

DOB based Model Predictive Voltage Control

Performance evaluation under parameter uncertainties

B. Low Voltage Distribution Network

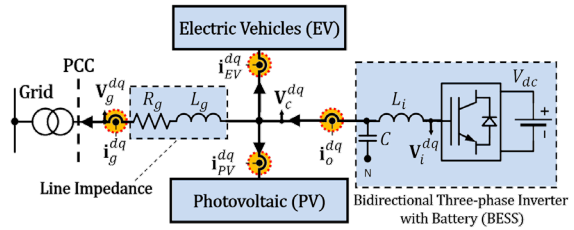

Fig. Electric vehicle charging station (EVCS) with line impedance in the low-voltage distribution network.

TABLE III
Uncertainty of line impedance

Experimental Case	R_g [Ohm]	L_g [mH]	μ
A-minimum ($1/\mu$)	0.8	1.06	1.25
B-minimum ($1/\mu$)	0.6	0.795	1.667
A-maximum (μ)	1.2	1.591	1.2
B-maximum (μ)	1.6	2.122	1.6

- CASE #3~4 : 2kW EV charging load with step input

Performance on $\mathbf{V}_c^{dq}$ voltage regulation

- *Experimental condition*

Exp. Case	R_g [Ohm]	L_g [mH]	μ
A-min. ($1/\mu$)	**0.8**	**1.06**	**1.25**
B-min. ($1/\mu$)	0.6	0.795	1.667
A-max. (μ)	1.2	1.591	1.2
B-max. (μ)	1.6	2.122	1.6

Exp. Case	R_g [Ohm]	L_g [mH]	μ
A-min. ($1/\mu$)	0.8	1.06	1.25
B-min. ($1/\mu$)	**0.6**	**0.795**	**1.667**
A-max. (μ)	1.2	1.591	1.2
B-max. (μ)	1.6	2.122	1.6

- *d-q* axis :

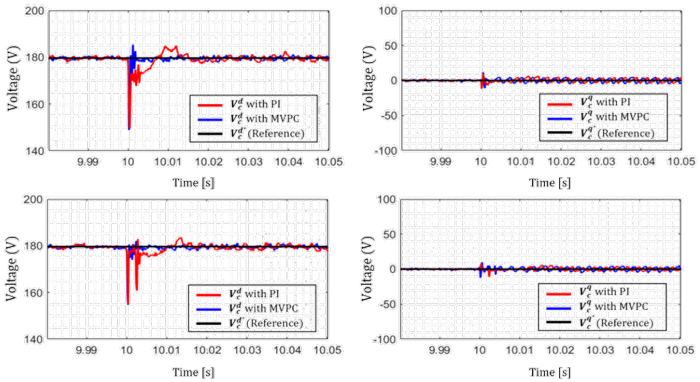

Fig. Comparisons of the performances of PI and MPVC when the 2kW EV charging load is applied to EVCS.

- CASE #5~6 : 2kW EV charging load with step input

Performance on $\mathbf{V}_c^{dq}$ voltage regulation

- *Experimental condition*

Exp. Case	R_g [Ohm]	L_g [mH]	μ
A-min. ($1/\mu$)	0.8	1.06	1.25
B-min. ($1/\mu$)	0.6	0.795	1.667
A-max. (μ)	**1.2**	**1.591**	**1.2**
B-max. (μ)	1.6	2.122	1.6

Exp. Case	R_g [Ohm]	L_g [mH]	μ
A-min. ($1/\mu$)	0.8	1.06	1.25
B-min. ($1/\mu$)	0.6	0.795	1.667
A-max. (μ)	1.2	1.591	1.2
B-max. (μ)	**1.6**	**2.122**	**1.6**

- *d-q* axis :

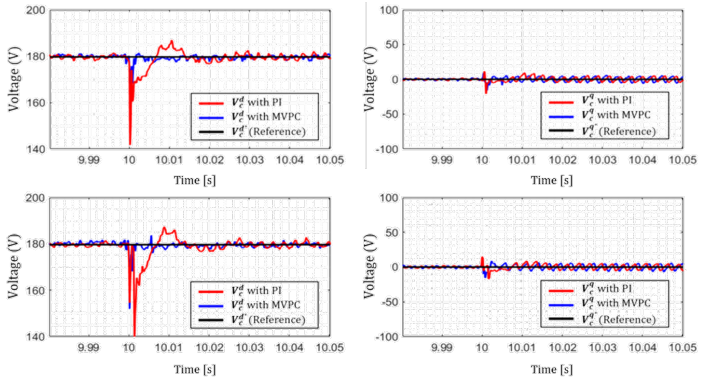

Fig. Comparisons of the performances of PI and MPVC when the 2kW EV charging load is applied to EVCS.

- CASE #7~8 : 2kW EV charging load with step input

- *Experimental condition*

Case	V_{AN}	V_{BN}	V_{CN}
CASE-A	**110.02 (86.6%)**	**127.02**	**127.02**
CASE-B	100.02 (78.7%)	127.02	127.02

Case	V_{AN}	V_{BN}	V_{CN}
CASE-A	110.02 (86.6%)	127.02	127.02
CASE-B	**100.02 (78.7%)**	**127.02**	**127.02**

- *d-q* axis :

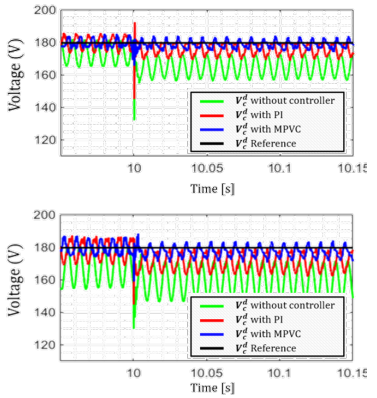

Performance on $\mathbf{V}_c^{dq}$ voltage regulation

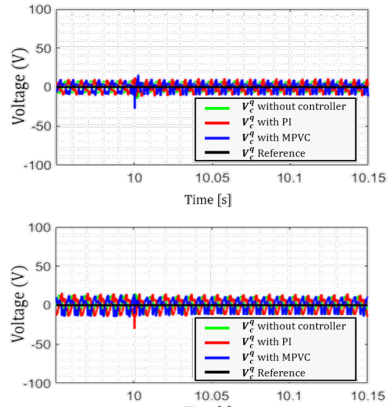

CONTENTS ...

UN environment programme | CTCN UN Climate Technology Centre & Network

GRIFFITH UNIVERSITY
SOCIAL MARKETING @ GRIFFITH

Antarctic Inland Microgrid Operation

RES-based Integrated and Control System for Extreme Environments

Establishment of a renewable energy supply system capable of replacing 30% of fossil fuel generation at the Antarctic inland base.

Development of optimal power grid operation technology based on diesel generators + renewable energy + energy storage systems, ensuring robustness and resilience.

Panoramic View of Jang Bogo Station(South Korea, Antarctica, opened at February 12, 2014)

Antarctic Inland Microgrid Operation

- **Average Wind Speed and Solar Irradiance in the Region between 60°S–90°S and 180°E–180°W**

	Spring (Oct.)	Summer (Dec./Jan.)	Autumn (Apr.)	Winter (Jul./Aug.)
Wind Speed $[m/s]$	1.14	0.975	0.98	1.41
Irradiation $[W/m^2]$	147.8	311.7	13.3	5.65

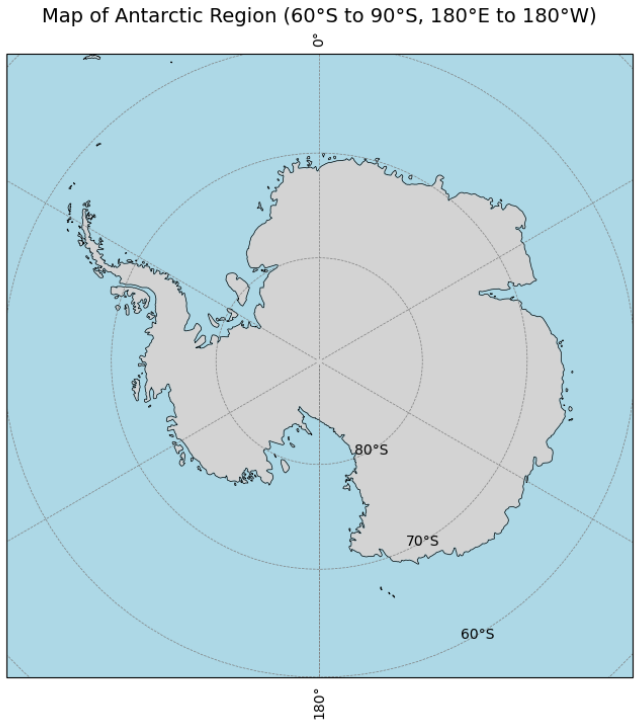

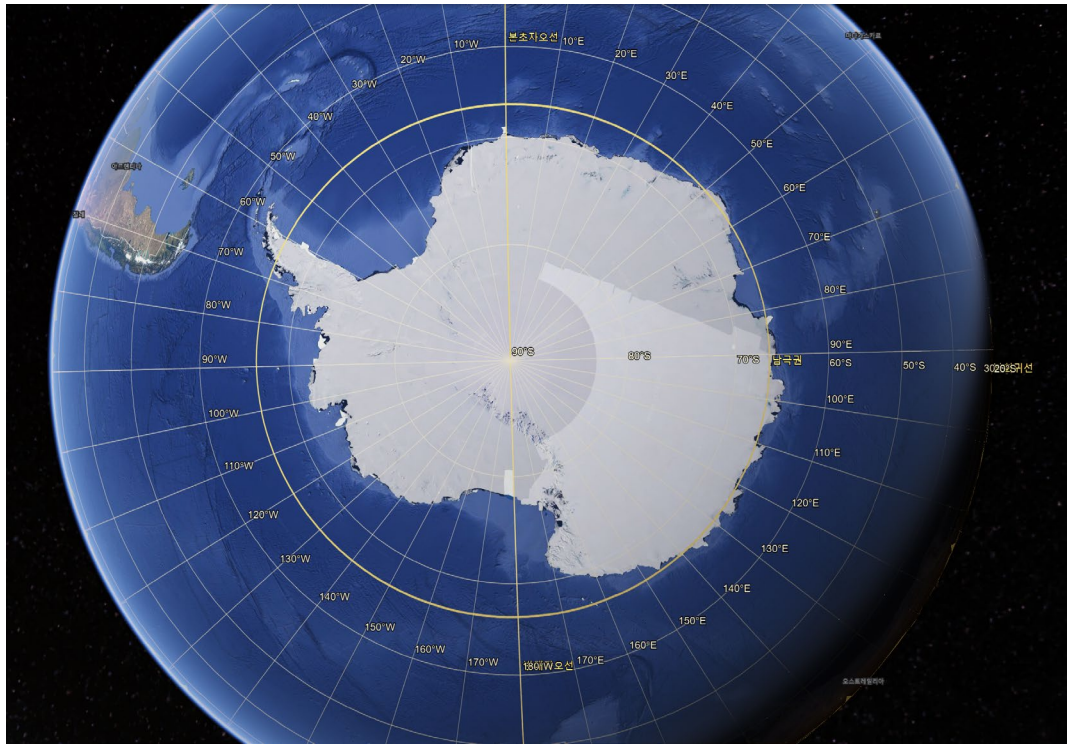

Antarctic Inland Microgrid Operation

- **Hourly Wind Speed Data (Mar 2023 ~ Feb 2024)**

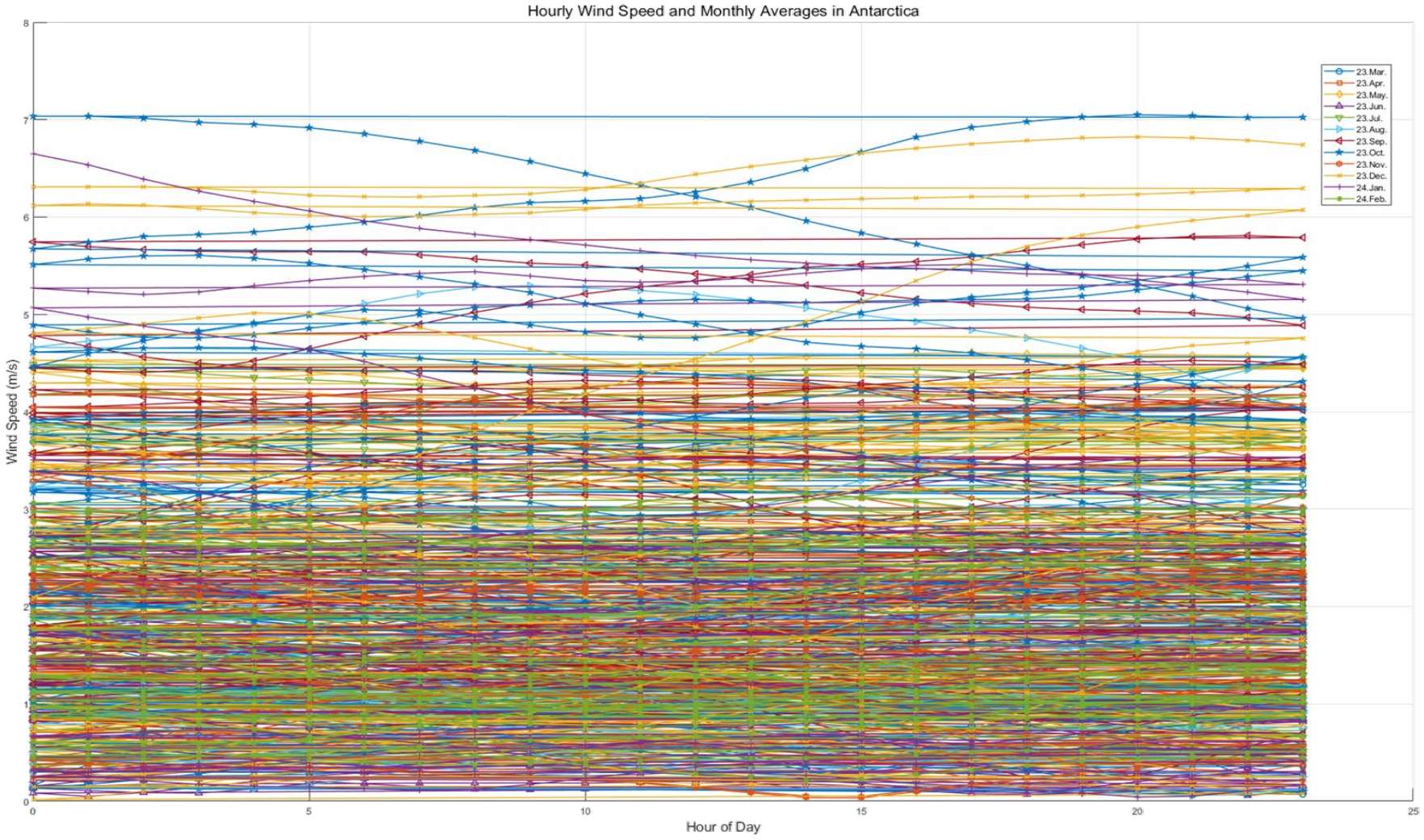

Antarctic Inland Microgrid Operation

- **Annual Wind Speed Data (2000 ~ 2024)**

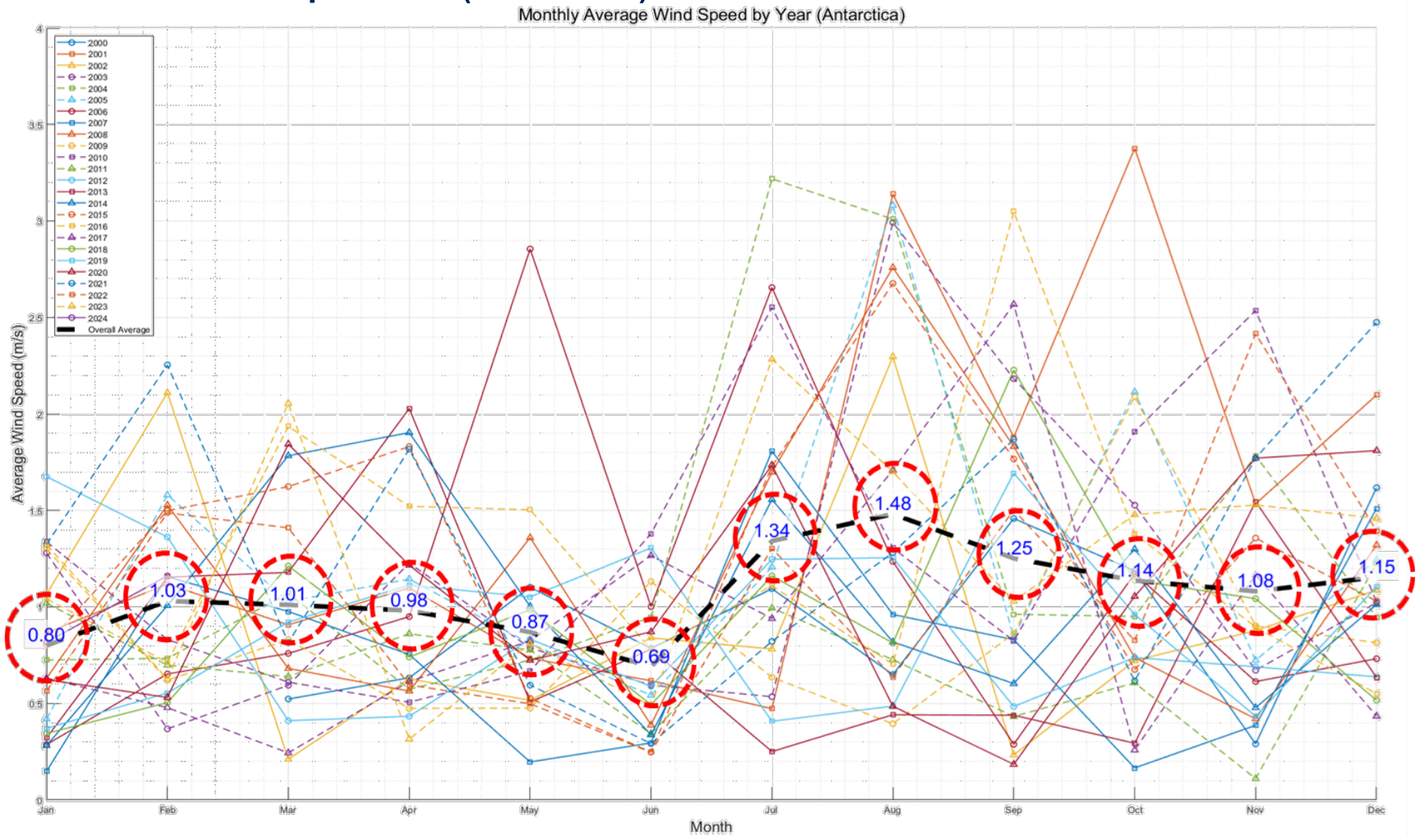

Antarctic Inland Microgrid Operation

- **Annual Solar Irradiance Data (2001 ~ 2024)**

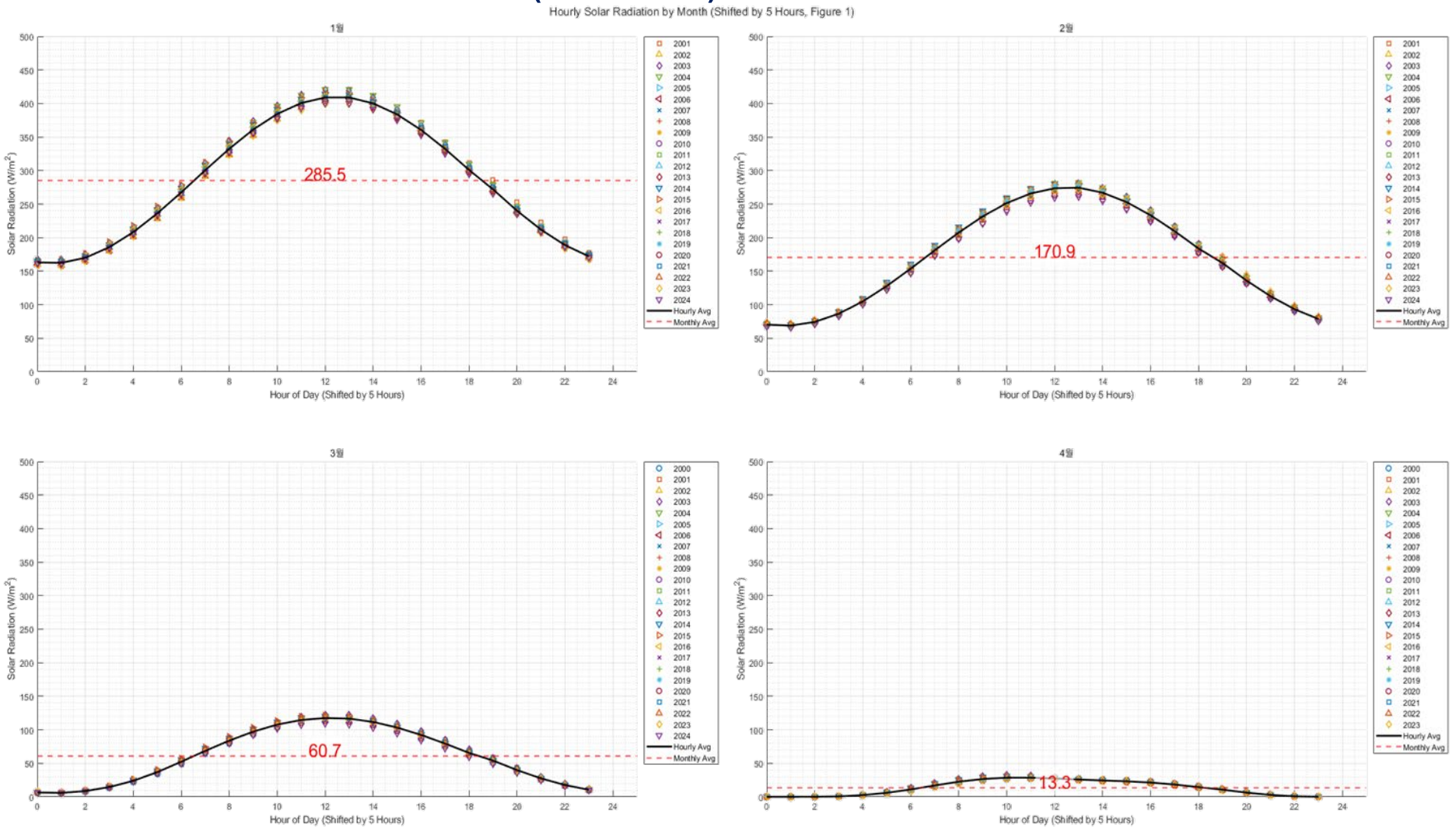

Antarctic Inland Microgrid Operation

- **Electric Power Usage Analysis of Station A / Station B**

  → Analysis Focused on Station B

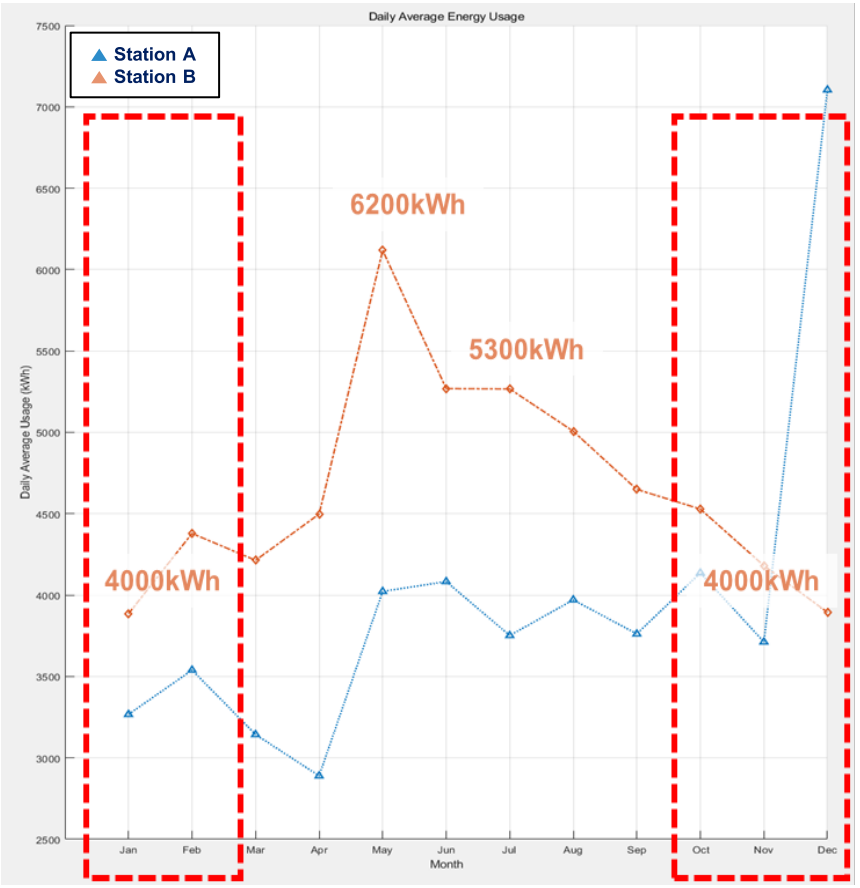

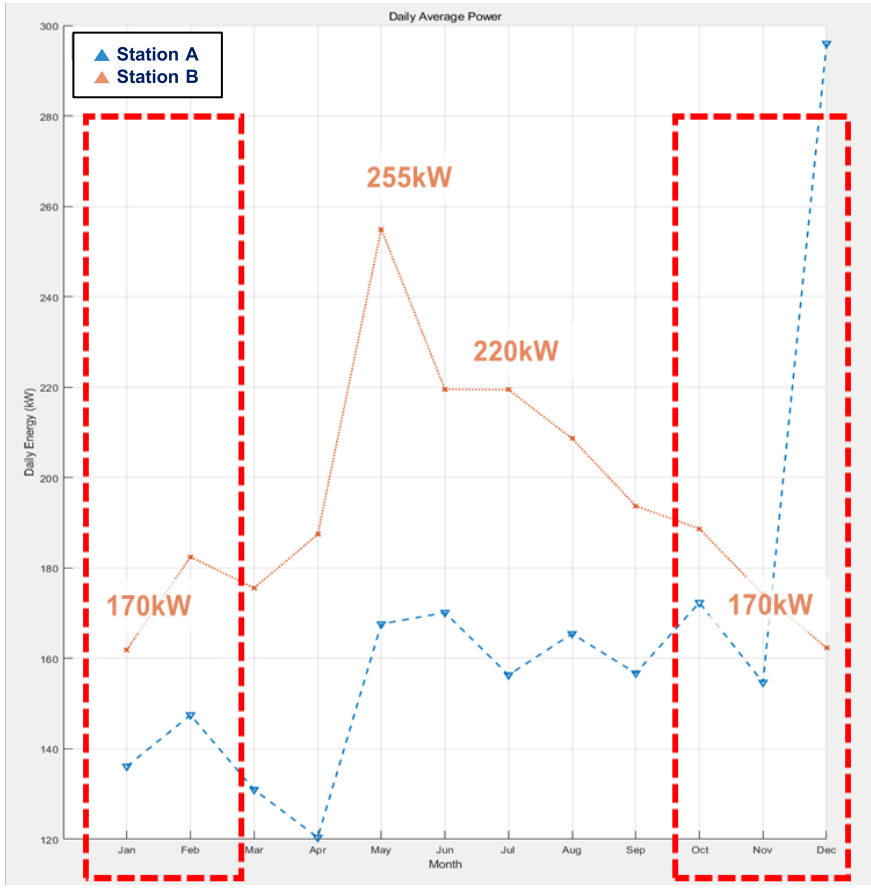

Antarctic Inland Microgrid Operation

Capacity Estimation for Achieving REx at the Antarctic Inland Station

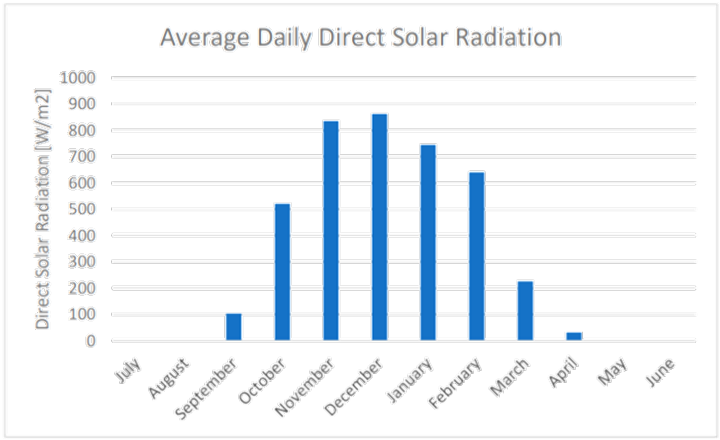

This figure shows the potential for PV installations from October till the end of February.
The graph is based on weather measurements at Concordia Station.

- Calculation of Average PV Generation in January (Daily based)

  (Overall efficiency of the PV system is assumed to be about 80%)

  - ✓ 10kW PV
    : 10kW x 24h x 0.75 x 0.8 = 144kWh
  - ✓ 50kW PV
    : 50kW x 24h x 0.75 x 0.8 = 720kWh
  - ✓ 100kW PV
    : 100kW x 24h x 0.75 x 0.8 = 1,440kWh

Maximum Power Demand of the Antarctic Inland Base (Daily based)

- Maximum power: 400 kW (Assumption, xxxx January)
- Maximum energy consumption: 4,000 kWh (xxxx January)
- Power / Energy : 400 kW / 4,000 kWh

Daily based RES Generation Ratio of the Antarctic Inland

- Instantaneous power (Max. RES / Max. Load)
  = 100kW / 400kW x 100% = 25.0%
- Renewable energy ratio (RES Energy / Load Energy)
  = 1,440kWh / 4,000kWh x 100% = 36.0% (RE36)

※ Values are simple calculations based on assumptions, for reference only.

※ Adjustable through the operation of Energy Storage Systems (ESS).

Source : de Witt, M.; Chung, C.; Lee, J. Mapping Renewable Energy among Antarctic Research Stations. Sustainability 2024, 16, 426

Antarctic Inland Microgrid Operation

Configuration of the Antarctic Inland Base Energy System

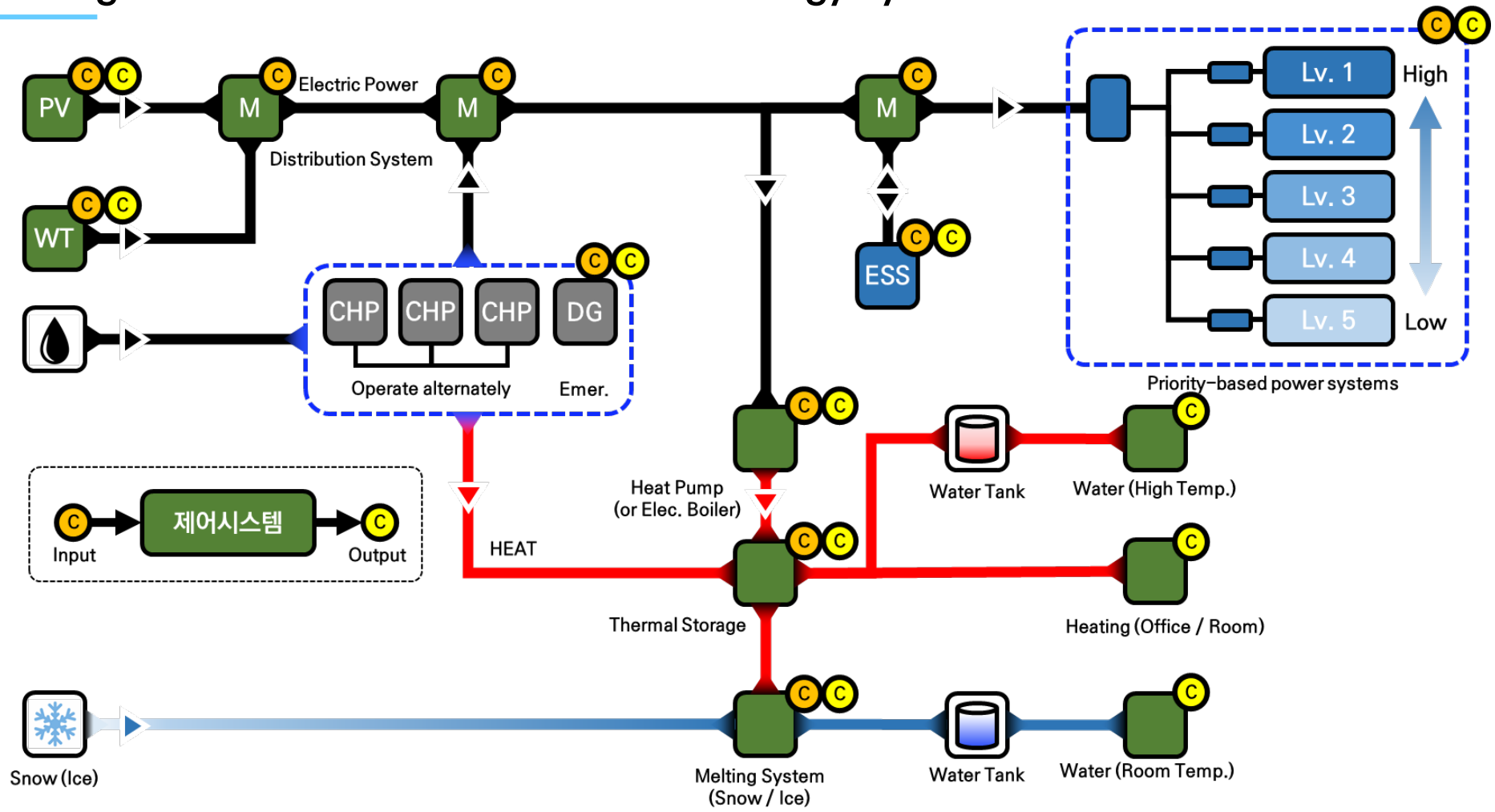

Antarctic Inland Microgrid Operation

Probabilistic Weighted Dispatch Framework for Polar Microgrids

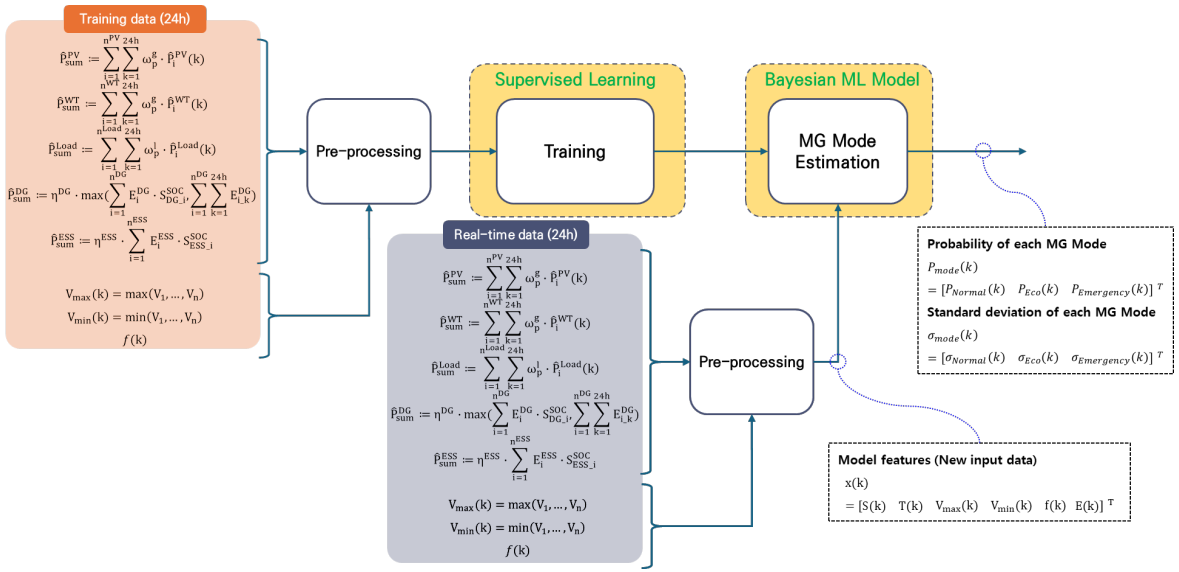

Normal mode :

→ Minimize the operating cost(economic dispatching)

$$\min_{u} J_N(\alpha) = \sum_{k=1}^{6h} \lambda_N^{WT}(\alpha) \cdot P^{WT}(k) + \sum_{k=1}^{6h} \lambda_N^{PV}(\alpha) \cdot P^{PV}(k) + \sum_{k=1}^{6h} \lambda_N^{DG}(\alpha) \cdot P^{DG}(k) + \sum_{k=1}^{6h} \lambda_N^{ESS}(\alpha) \cdot P_{Dis}^{ESS}(k) + \sum_{k=1}^{6h} \lambda_N^{ESS}(\alpha) \cdot P_{Ch}^{ESS}(k) + \cdots$$

Eco mode :

→ Minimize the diesel generator output, Increase self-sufficiency, minimize diesel fuel consumption for extended operation, and implement load shedding

$$\min_{u} J_C(\beta) = \sum_{k=1}^{6h} \lambda_N^{DG}(\beta) \cdot P^{DG}(k) + \sum_{k=1}^{6h} \lambda_N^{ESS}(\beta) \cdot P_{Dis}^{ESS}(k) + \sum_{k=1}^{6h} \lambda_N^{ESS}(\beta) \cdot P_{Ch}^{ESS}(k) + \sum_{i=1}^{n} \sum_{k=1}^{6h} \lambda_{N,i}^{Shed}(\beta) \cdot P_i^{Shed}(k) + \cdots$$

Emergency mode :

→ Start a high-reliability operation mode by curtailing renewables, increasing reliable generation (diesel generators, ESS), and shedding loads if needed.

$$\min_{u} J_E(\gamma) = \sum_{k=1}^{6h} \lambda_N^{DG}(\gamma) \cdot P^{DG}(k) + \sum_{k=1}^{6h} \lambda_N^{ESS}(\gamma) \cdot P_{Dis}^{ESS}(k) + \sum_{k=1}^{6h} \lambda_N^{ESS}(\gamma) \cdot P_{Ch}^{ESS}(k) + \sum_{i=1}^{n} \sum_{k=1}^{6h} \lambda_{N,i}^{Shed}(\gamma) \cdot P_i^{Shed}(k) + \cdots$$

- Proposed control method

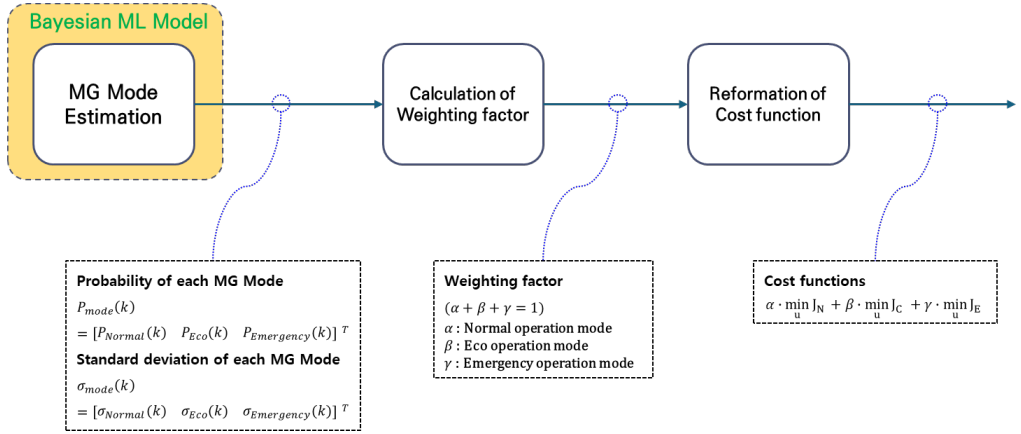

Antarctic Inland Microgrid Operation

Probabilistic Weighted Dispatch Framework for Polar Microgrids

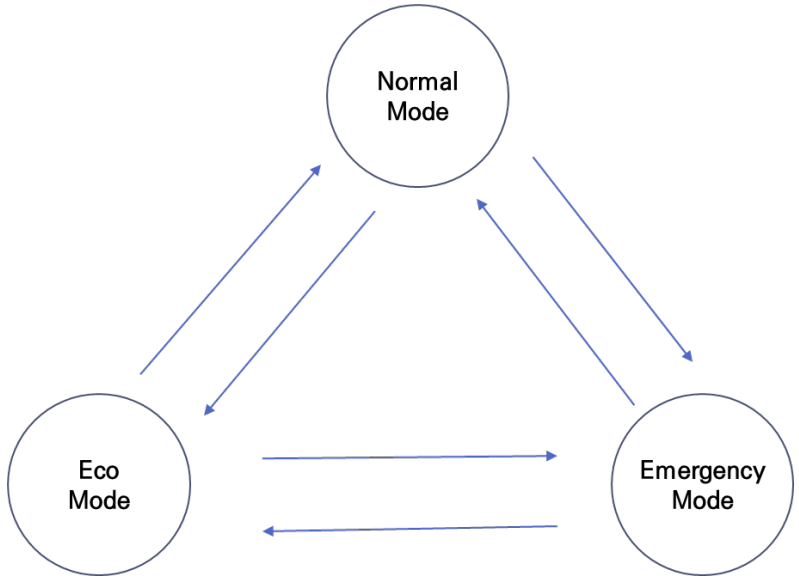

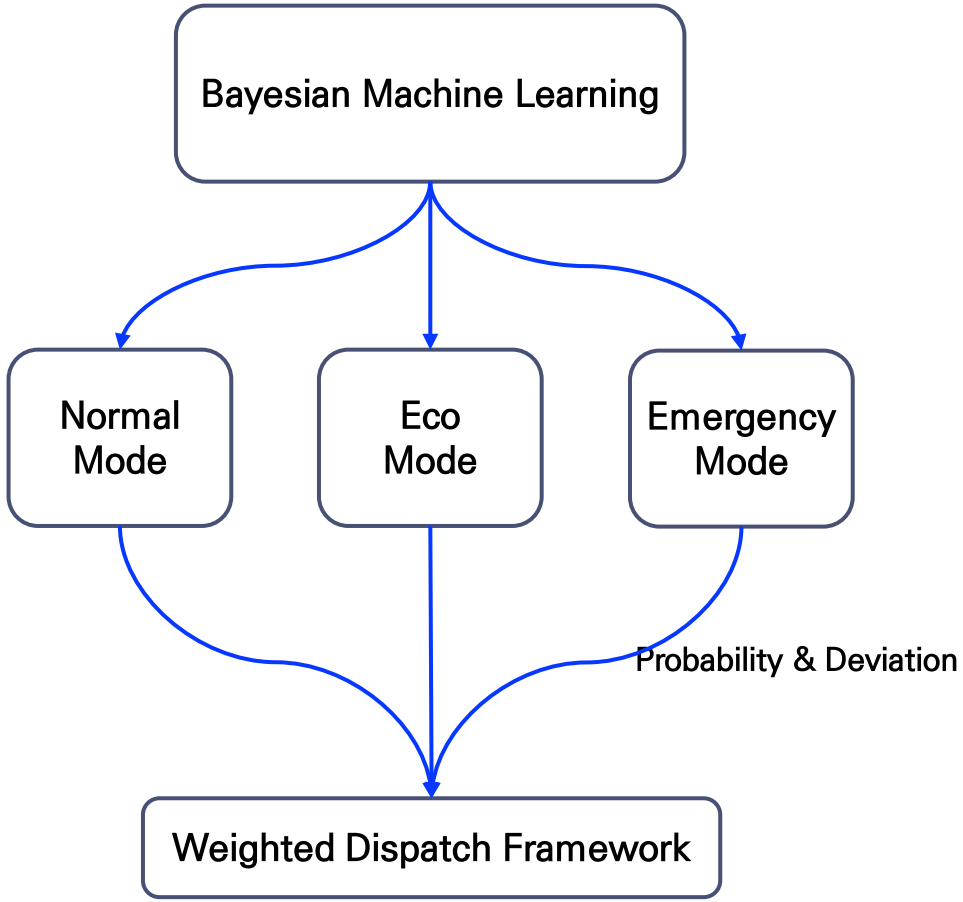

$(\alpha + \beta + \gamma = 1)$

Antarctic Inland Microgrid Operation

Probabilistic Weighted Dispatch Framework for Polar Microgrids

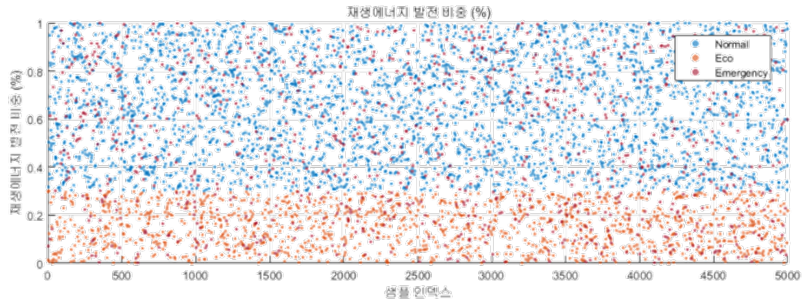

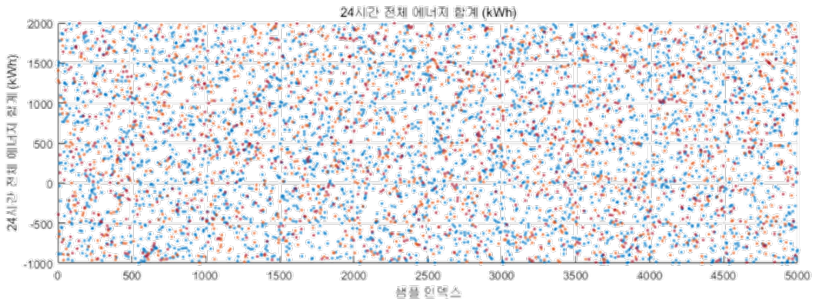

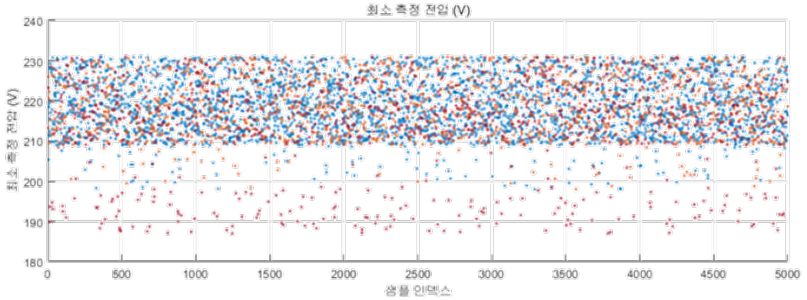

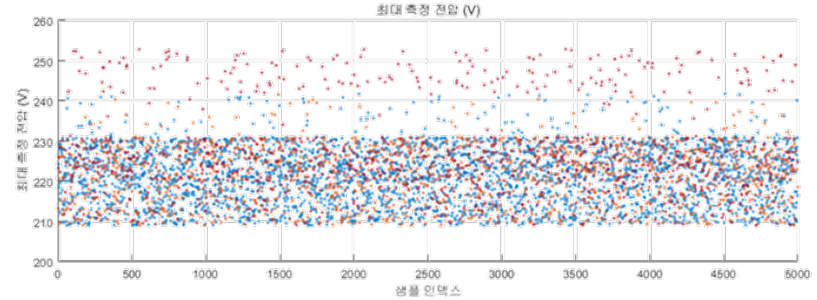

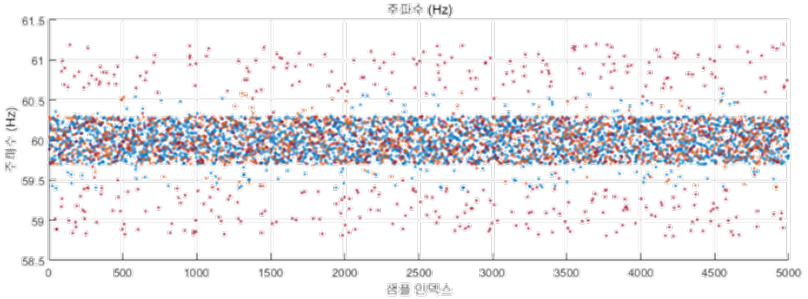

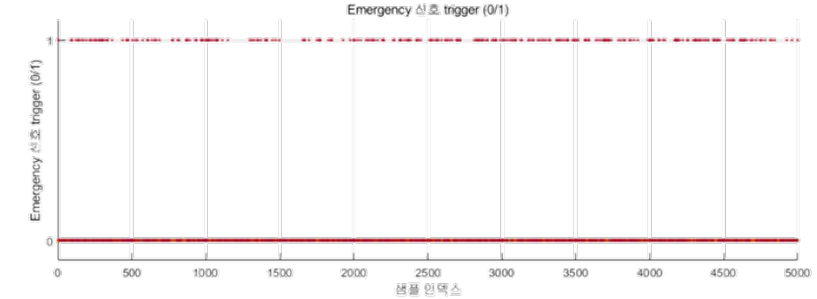

Antarctic Inland Microgrid Operation

Probabilistic Weighted Dispatch Framework for Polar Microgrids

Model features (New input data)

$$x(k) = [S(k) \quad T(k) \quad V_{max}(k) \quad V_{min}(k) \quad f(k) \quad E(k)]^{T}$$

x_test = [0.2, 1200, 215, 225, 59.9, 0];

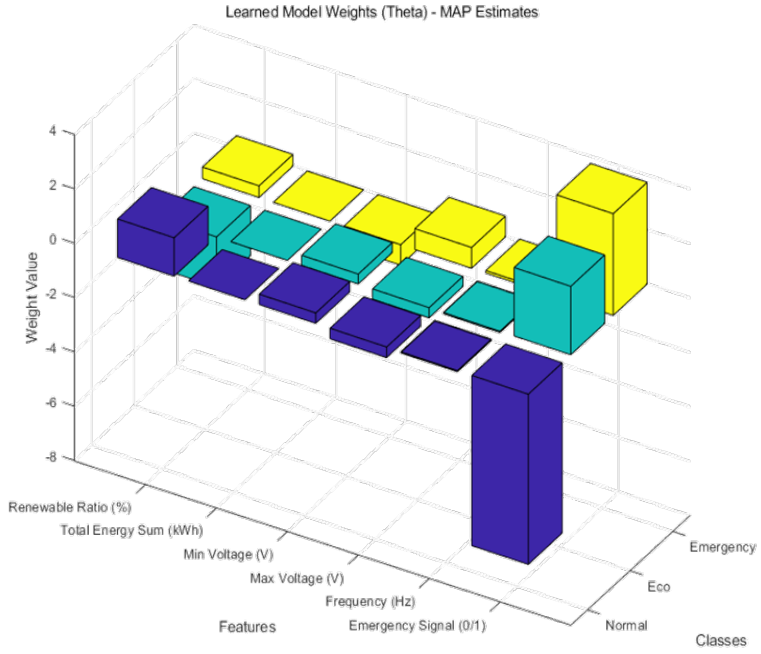

Estimation Results of High–Probability Values in the Posterior Probability Distribution of Model Parameter θ

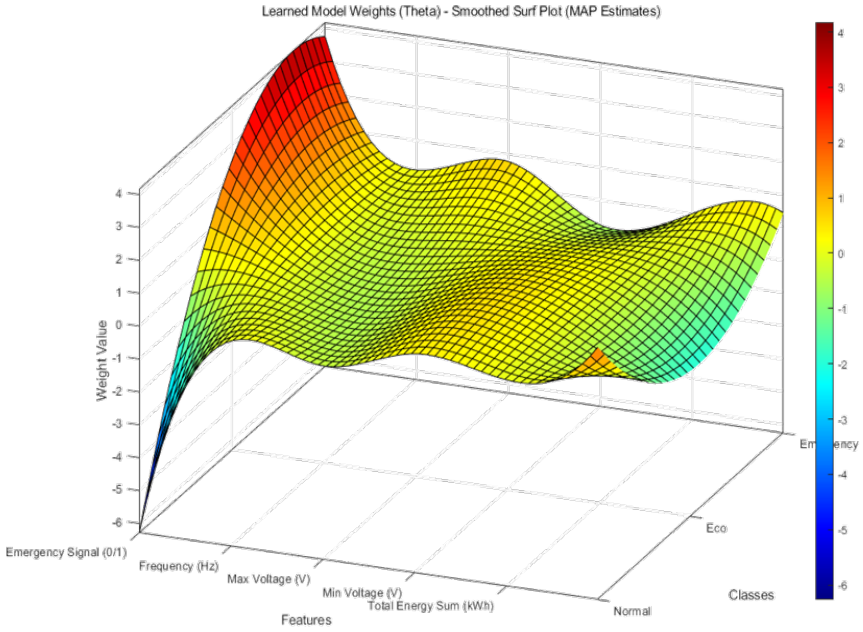

3D Surface of High–Probability Estimates for the Posterior Distribution of Model Parameter θ

Antarctic Inland Microgrid Operation

Probabilistic Weighted Dispatch Framework for Polar Microgrids

Estimation Results for New Input Data :

$$P(Y_{new}|X_{new}, X, Y) = \int P(Y_{new}|X_{new}, \theta)P(\theta|X, Y)d\theta$$

x_test = [0.2, 1200, 215, 225, 59.9, 0];

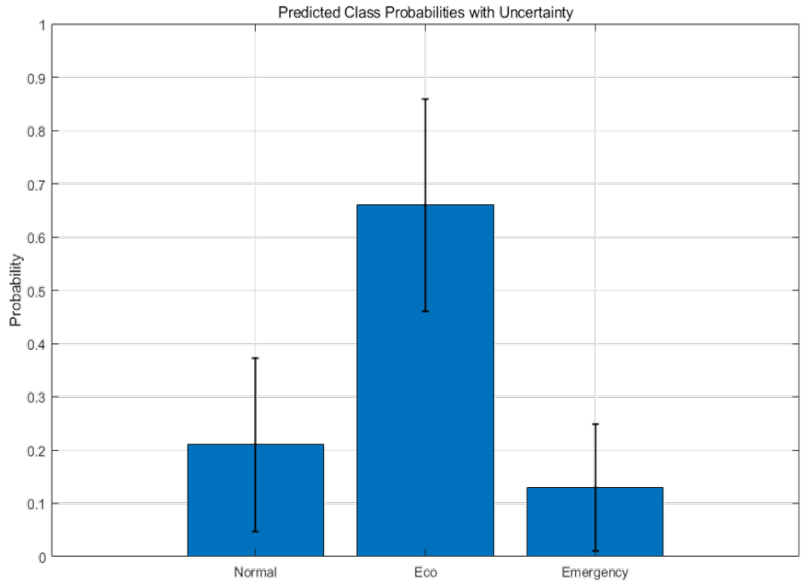


```
명령 창
  Training data preparation complete. Number of samples: 10000, Features: 6
  Starting MAP estimation...
  MAP estimation complete.
  Calculating Hessian and covariance matrix...
  Laplace Approximation complete.
  Predicting for new test data: [0.2          1200          215          225          59.9            0]
  Logit uncertainty calculated.
  Monte Carlo sampling complete.

  📌 예측 결과 (Bayesian Multiclass Logistic Regression)
  Normal Mode: Mean = 0.210, Std = 0.162
  Eco Mode: Mean = 0.660, Std = 0.200
  Emergency Mode: Mean = 0.130, Std = 0.119
```

```
Calculating weighting factors...
Calculated raw weights (lambda = 1.00):
  W_Normal: 1.2922
  W_Eco: 3.2273
  W_Emergency: 1.1109

Final Normalized Weighting Factors:
  alpha (Normal Mode): 0.2295
  beta (Eco Mode): 0.5732
  gamma (Emergency Mode): 0.1973
Sum of weighting factors: 1.0000
```

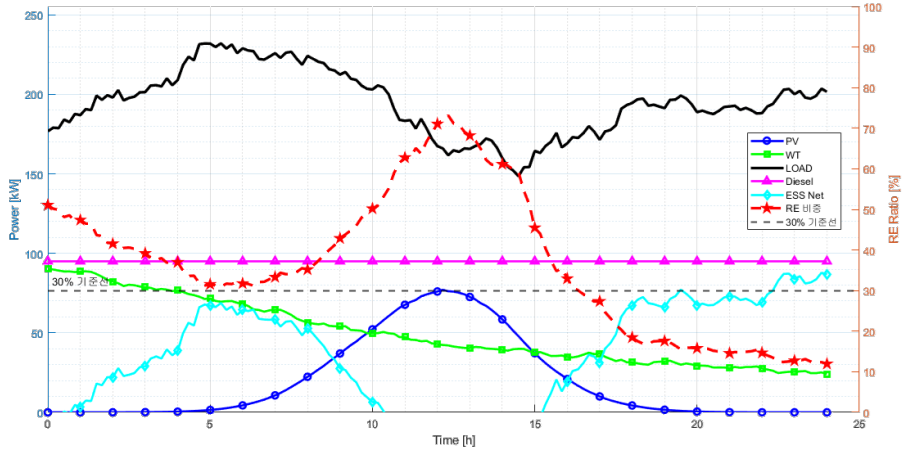

Simulation results under the probability variations of microgrid operating modes

Antarctic Inland Microgrid Operation

Antarctic Inland Microgrid Operation (GFM : Grid Forming)

RES-based Integrated and Control System for Extreme Environments

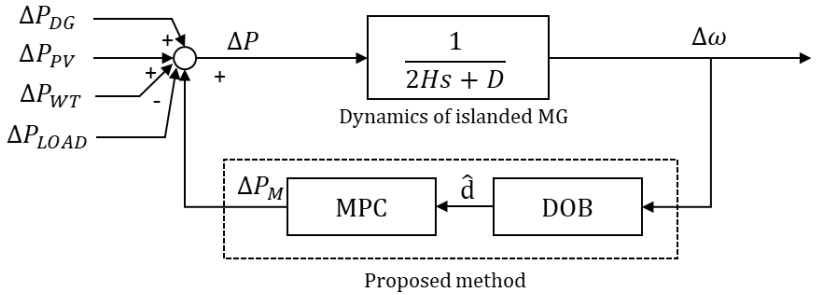

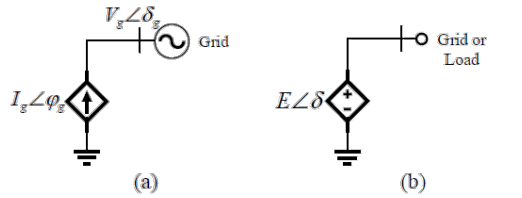

Fig. 1. Simplified representation of power converters.
(a) Grid-following converter; (b) Grid-forming converter.

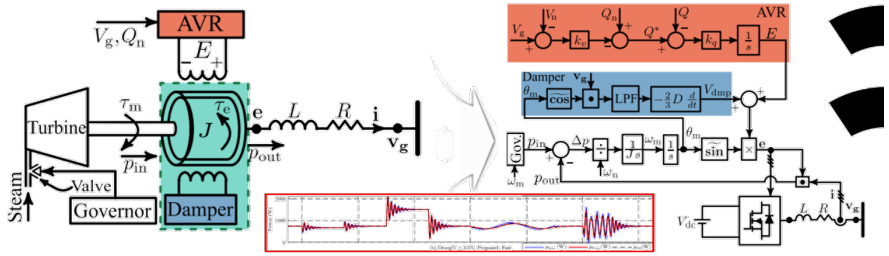

M. Ebrahimi et. al., "An Improved Damping Method for Virtual Synchronous Machines," IEEE Trans. Sustain. Energy, 2019.

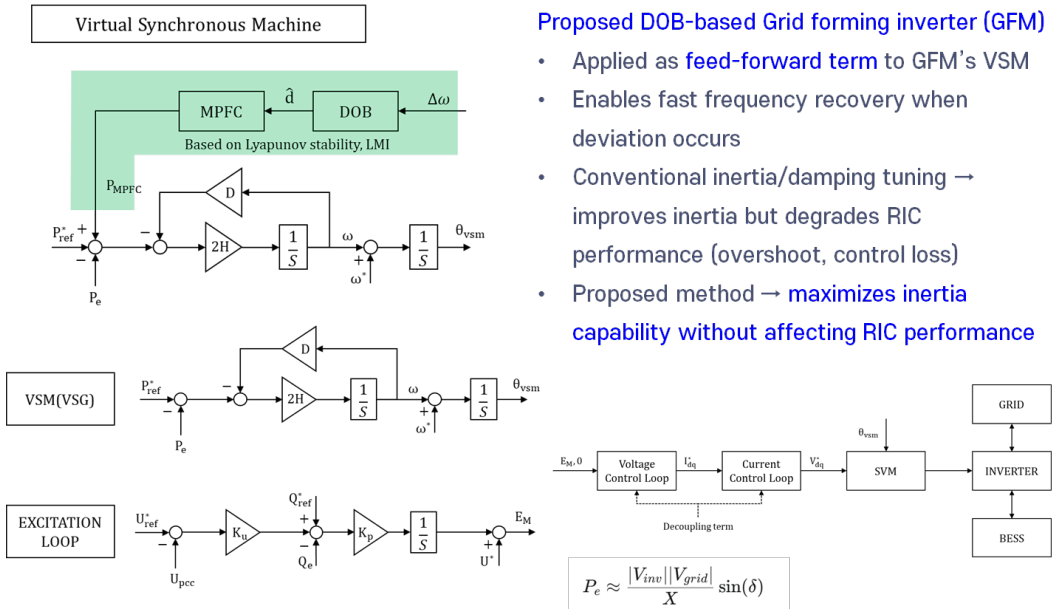

Proposed DOB-based Grid forming inverter (GFM)

- Applied as feed-forward term to GFM's VSM
- Enables fast frequency recovery when deviation occurs
- Conventional inertia/damping tuning → improves inertia but degrades RIC performance (overshoot, control loss)
- Proposed method → maximizes inertia capability without affecting RIC performance

$$P_e \approx \frac{|V_{inv}||V_{grid}|}{X}\sin(\delta)$$

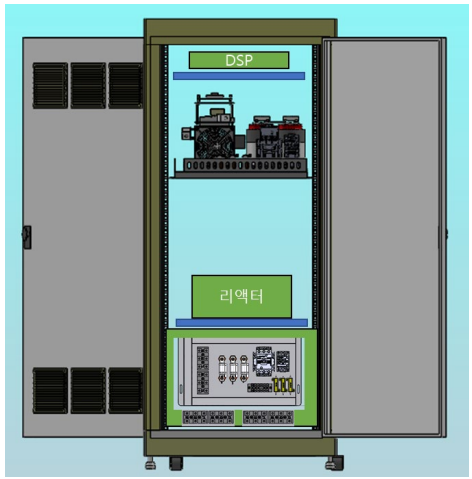

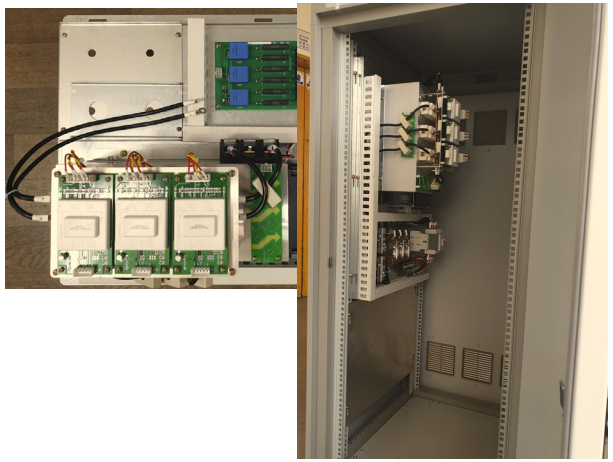

The DOB–based MPC–GFM inverter is currently under development.

Antarctic Inland Microgrid Operation

Development of a Pre-verification System for Microgrid Operation

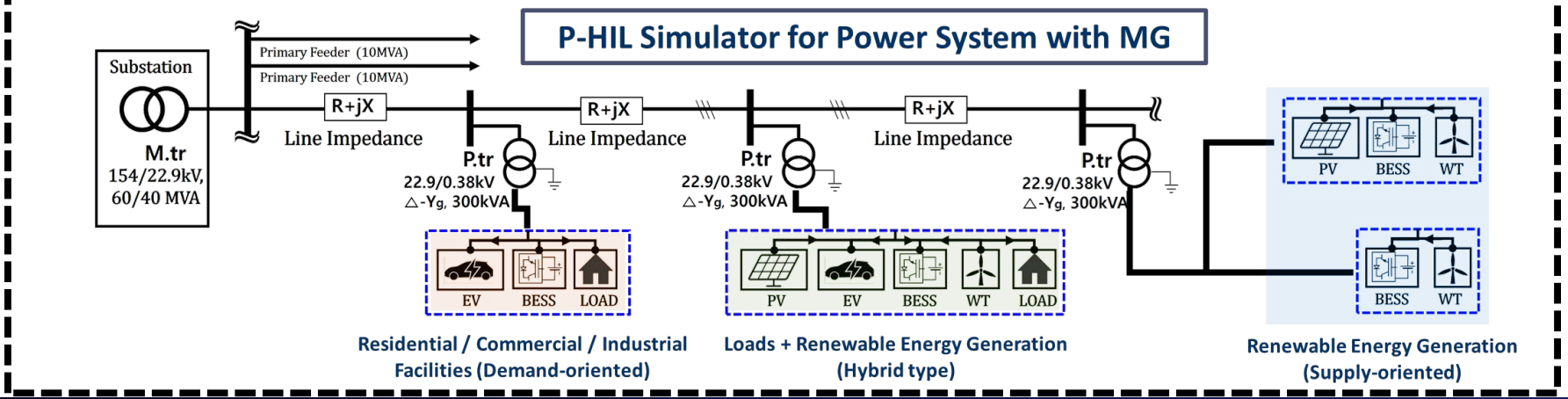

Antarctic Inland Microgrid Operation

Development of a Pre-verification System for Microgrid Operation

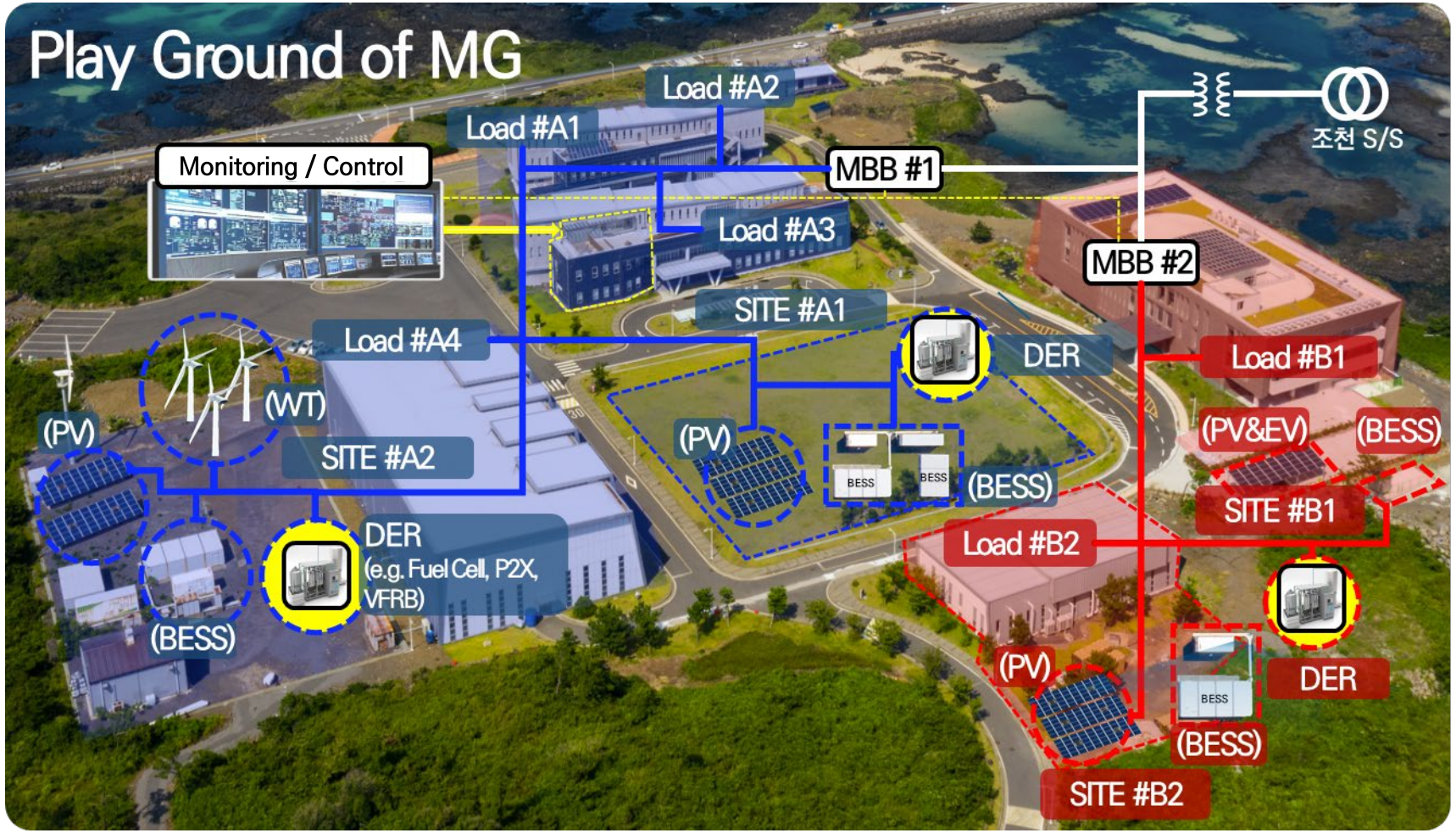

Thank you for your attention!

Dae-Jin Kim, Ph.D
Chief(Principal Researcher)
Electric Power System Research Lab.
Korea Institute of Energy Research
djk@kier.re.kr
+82-10-3395-4383